Energy Reports 8 (2022) 5541–5561

Contents lists available at ScienceDirect

Energy Reports

journal homepage: www.elsevier.com/locate/egyr

Research paper

Risk-based maintenance strategy selection for wind turbine composite blades

Javier Contreras Lopez, Athanasios Kolios *

Naval Architecture, Ocean & Marine Engineering, University of Strathclyde, 16 Richmond St, Glasgow – G1 1XQ, Scotland, UK

ARTICLE INFO

Article history:
Received 14 September 2021
Received in revised form 1 March 2022
Accepted 7 April 2022
Available online xxxx

Keywords:
Wind turbine blades
Risk assessment
Maintenance strategy
FMEA

ABSTRACT

Blades are one of the most important components, in terms of capital and operational costs, of wind turbines. In contrast with some other elements of the turbine, the knowledge regarding the failure modes and processes of the composite materials that form the blade are less known. Therefore, providing a systematic study breaking down the individual components of the blade and analysing the criticality of each of the failure modes affecting them is the first step toward the implementation of measures reducing operational and maintenance costs. The scarce information that is publicly available regarding wind turbine blade failures and their constant evolution inclines risk analysis toward studies based on expert opinion. In this study, the criticality of the failure modes is determined through a failure mode and effects analysis (FMEA) that examines the severity and likelihood of occurrence of the failure modes identified. In light of the results of criticality, the current and potential maintenance strategies covering the different failure modes will be identified, along with the applicable monitoring techniques found in the literature, to propose risk mitigation strategies. The results of this study may be utilized for further exploration of operation and maintenance analysis toward the development of dynamic decision support systems.

1. Introduction

Wind is one of the prevailing energy sources to generate electricity today. The environmental advantages that this source provides are aligned with the world policies targeting carbon neutrality and, along with the cost reduction that it has experienced lately (IEA, 2020), it has become one of the preferred energy sources. Some well known policies promoting the use of renewable energy are those promoted by the EU which targets increasing the use of renewable energy to 27% of the total energy generation by 2030, and cutting greenhouse emissions by 80%–95% by the year 2050 (Corbetta et al., 2015), and the United States with a target of 20% of wind-generated electricity (Wilburn, 2011). Also, China has experienced an increase of 27% in growth rate of the electricity generated from wind between 2016 and 2017 (Global Wind Energy Council (GWEC), 2018). The installed wind capacity reflects the favourable context for wind energy harvesting. The sharp increase of worldwide installed wind turbines capacity experienced, from 180,846 MW in 2010 to 733,276 MW in 2020 (International Renewable Energy Agency (IRENA), 2021), is expected to continue its expansion in the upcoming decades.

To continue with this trend, the reduction of capital and operational costs is essential. In this sense, several offshore wind turbine life costs analyses have revealed that operation and maintenance (O&M) costs can represent up to more than 30% of the total costs of wind turbines throughout their life (Stehly and Beiter, 2020; Martin et al., 2016). Furthermore, turbine blades along with the gearbox and electrical generators have been identified as the components with the greater failure rates of the turbines (Li et al., 2018; Tautz-Weinert and Watson, 2016). In contrast with gearboxes, electrical generators and other components, where the use of condition monitoring is much more mature and is currently implemented in some turbines (Martinez-Luengo et al., 2019; Black et al., 2021; Nejad et al., 2014; Shen et al., 2018; Dewangan et al., 2020), the blades are rarely instrumented and their inspections and maintenance are usually calendar-based which creates an opportunity for improvement on their reliability and life extension by switching to condition-based types of maintenance (Martinez-Luengo et al., 2016; Kolios and Martínez-Luengo, 2016).

To determine which failure modes are more relevant and drive the reliability of the blades, a systematic analysis is provided in this study by means of a comprehensive Failure Modes and Effects Analysis (FMEA). In this analysis, the severity and occurrence of each of the failure modes will be considered so as to define a criticality number (*CN*). Based on the resulting *CN*, risks will be prioritized to study the implementation of improved

* Corresponding author.
E-mail address: athanasios.kolios@strath.ac.uk (A. Kolios).

https://doi.org/10.1016/j.egyr.2022.04.027

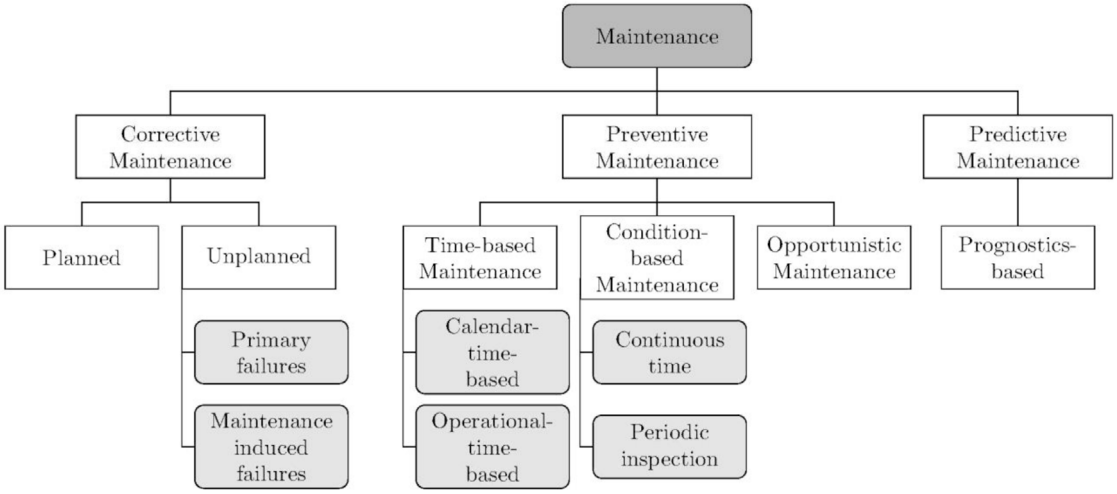

Fig. 1. Types of maintenance.
Source: Adapted from Kolios (2020).

maintenance and inspection strategies. The types of maintenance under consideration are shown in Fig. 1. Conceptually, there is a big difference from corrective maintenance or statistics-based preventive maintenance to condition-based maintenance based on non-destructive testing or sensor data. As opposed to corrective and statistics-based preventive maintenance, condition-based maintenance requires a deep knowledge of the failure mode under study.

Later, the current maintenance strategy usually applied for the failure modes will also be indicated. Following this, the feasibility of detection of each failure mode along with the feature or features and structural health monitoring (SHM) techniques used for its detection will be explored among the existing literature. Finally, the maintenance decision framework proposed in Kolios (2020) will be used toward the development of a risk policy to determine a feasible maintenance strategy for each of the blade failure modes above a considerable risk threshold to enhance the current practice and impact in the overall reliability of the blade. This study will also serve as a guide for the main failure modes to be included in wind turbine blade O&M modelling for an effective representation of the physical system. In contrast with existing risk analysis of wind turbine components where the criticality of different components is presented, this study analyzes in detail the failure modes at component level for the blades, providing a detailed vision of the nature and effects of the failure modes and a risk policy for the selection of the optimal inspection and maintenance strategy. Transitioning from predetermined or corrective maintenance to condition-based maintenance can report an increased availability of the assets if properly performed (Koukoura et al., 2021). Therefore, this study provides the natural step forward to commence the implementation of practices to increase the reliability of wind turbines and could be used by wind farm operators and other stakeholders as a guide for other components (tower, generator, drivetrain, …).

2. Literature review

When facing the problem of increasing the reliability of a system, the concept of risk is widely used in the prioritization of components and failure modes. It is defined in ISO 31000 (Standard and Standard, 2009b) as *the effect of uncertainty on objectives*. A concept closely related to risk in O&M management is criticality. Both concepts combine the likelihood of an undesired event happening with the severity of its consequences (usually environmental, economic and safety), being the criticality used to provide a prioritization of failure modes within a system (Standard, 2001). Among the existing qualitative and quantitative methods to prioritize failure modes of systems presented in the ISO 31000 series of standards (Standard and Standard, 2009b,a), the Failure Mode and Effect Analysis (FMEA) and its extension, the Failure Mode Effects and Criticality Analysis (FMECA) that incorporates the analysis of the criticality of the failure modes of the system, have been extensively applied in the operation of physical assets in particular. Risk prioritization studies such as the one provided in this manuscript call for qualitative or semi-quantitative approaches in the absence of a significant amount of date. In this sense, the FMEA has been selected as the method for this study to overcome the lack of data with the data required to individually characterize the identified failure modes. In the future, the application of quantitative methods like the ones proposed in ISO 2394 (Standard and Standard, 2015) will improve informed O&M decision-making for wind turbine blades. A comprehensive review of the different risk and reliability-based analysis can be found in Leimeister and Kolios (2018). The IEC 60812 standard (International Electrotechnical Commission et al., 2018) describes in a comprehensive way the steps for the application of the FMEA and the FMECA. The strength of these methods comes from its versatility to accommodate quantitative and qualitative data, and therefore the combination of physics-based and data-based knowledge, while preserving a logical and structured approach.

During the last decade, there have been several risk assessment studies considering the complete wind turbine (Arabian-Hoseynabadi et al., 2010; Shafiee and Dinmohammadi, 2014a; Dinmohammadi and Shafiee, 2013; Das et al., 2011; Ozturk et al., 2018; Li et al., 2020; Magomedov et al., 2019; Scheu et al., 2019; Luengo and Kolios, 2015; Shafiee and Dinmohammadi, 2014b). Considering the different environments to which wind turbines are exposed, the comparison of failure modes between onshore and offshore wind turbines was studied in Shafiee and Dinmohammadi (2014a), showing that risk and cost increase for offshore turbines while the risk rank of components is fairly consistent. In Li et al. (2020), a two-stage FMECA considering 13 components including the blades is presented in which blades are the most relevant component in terms of a combination of cost and risk priority. In Magomedov et al. (2019), an FMEA and a failure mode maintenance analysis are presented in which six

Table 1
Risk and reliability studies including wind turbine blades in the literature.

Reference	Blade included	Number of blade failure modes	Failure modes
Arabian-Hoseynabadi et al. (2010)	Yes	4	Mechanical rupture, fracture, detachment, fatigue
Li et al. (2020)	Yes	3	Blade cracks, delamination, gear teeth slip (rotor)
Magomedov et al. (2019)	Yes	2	Crack in blade, gear teeth slip (rotor)
Scheu et al. (2019)	Yes	19	Cracks, delaminations, debonding, top coat damage, lightning damage
Luengo and Kolios (2015)	Yes	12	Cracks, delaminations, surface wear, increased surface roughness, fatigue, lightning strikes, high vibrations, flapwise fatigue damage, unsteady blades air loads, blade fracture, unsteady performance, corrosion
Shafiee and Dinmohammadi (2014b)	Yes	7	Abnormal vibration, blade surface roughness, bird crash, ice-forming, hurricane, earthquake, wrong materials

components, including the blades, are also analysed. Arabian-Hoseynabadi et al. (2010) performed an FMEA of the wind turbine and compared it with reliability field data and suggested further analysis at the component level. Scheu et al. (2019) performed an analysis based on an in-depth FMECA study in which 337 failure modes were identified and analysed by experts. Additionally, the potential benefit of deploying monitoring systems was assessed for the critical failure modes. Separately, Luengo and Kolios (2015) reviewed the main failure modes of wind turbines found in the literature to provide a view on end of life scenarios for different components.

Notwithstanding the proliferation of different risk and reliability analysis of wind turbines, to the best of the authors' knowledge, the existing studies are focused on the identification and prioritization of wind turbine components without the detail required to propose individual monitoring techniques and maintenance strategies for the most critical failure modes. This additional step is essential for the implementation of improvements in the system. Table 1 summarizes some of the studies found in the literature in which the blades or rotor were studied. In order to challenge the current maintenance practice, a detailed risk assessment at component level is deemed necessary. Thus, understanding and evaluating the impact of each of the failure modes of wind turbine blades is the first step toward the implementation of new practices for reliability improvement of this component.

3. Developing a risk-based maintenance strategy selection policy

The stakeholders of the industry are seeking important cost reductions in the maintenance of wind energy assets. In this sense, the analysis of the reliability of the different components and the selection of the optimum maintenance strategy or combination of maintenance strategies are not trivial problems. Developing a risk policy and, therefore, assigning thresholds to target failure modes is a critical task to bring down these costs. In contrast with much more mature industries such as the automotive or offshore Oil&Gas which have developed standardized risk policies based on accumulated knowledge and data, the wind industry and, in particular the offshore wind industry, are in need of more studies.

In this study, the scope of the FMEA will be the blade, and it will be broken down into the following components as seen in Fig. 2 (upper and bottom shell, spar, root, and the leading and trailing edges). The first step of the analysis is the identification of the failure modes, which are the manners in which failures can occur. Secondly, the effects or consequences of the failures will be presented. Furthermore, the causes initiating them and the failure mechanisms that are developed toward the failure will also be identified. The criticality will be assessed using a 2-parameter approach that will define the criticality number (CN). The CN will be computed as follows:

Table 2
Severity factor categorization.

Category	Description	Factor
Negligible	Unidentifiable or only cosmetic damage	1
Minor	Damage not causing interference with the normal operation of the wind turbine	2
Moderate	Damage having slight consequences to the operation of the turbine but not causing service disruptions	3
Major	Damage interfering with the operation of the wind turbine and causing service disruptions	4
Catastrophic	Failure of the system	5

$$CN = S \cdot O \tag{1}$$

where S is the Severity (relative ranking of potential or actual consequences of a failure) and O is the Occurrence (relative likelihood of the occurrence of a failure) factor. The range of values considered for these factors spans from 1 to 5 according to the criteria shown in Tables 2 and 3. The values of Occurrence have been set in agreement with the studies shown in Table 1 and expert elicitation. Separately, the values of Severity, have been chosen considering the economic and structural implications of the development of the failure mode. As defined for this work, occurrence and severity factors have equal weight toward the criticality of the failure mode. The values for the resulting criticality range from 1 for the less critical mode to 25 for the most critical. The criticality domain has been divided into four categories (low, moderate, high and extreme) as shown in the matrix of Fig. 4. The guidelines presented in Anthony (Tony) have been carefully considered as to provide a risk matrix with sufficient resolution and to balance ratings so that negatively correlated frequency and severity values of the identified failure modes can provide insightful criticality numbers. The approach used for this study is in line with recent relevant papers in the same field, such as Scheu et al. (2019) and Kolios (2020). While other studies include a third factor called Beta factor or detectability, which represents the conditional probability of the failure end effect to materialize given that the failure mode has occurred, only Severity and Occurrence have been considered to use the risk matrix as an approach for risk visualization and acceptance. This practice is widely used in industry through relevant standards and risk policies. In this study, failure modes with a criticality of high or above will be prioritized to propose monitoring and maintenance strategies for the reduction of their criticality.

After the classification of failure modes according to the proposed CN, this study provides a systematic framework for maintenance strategy selection following the decision tree in Fig. 3.

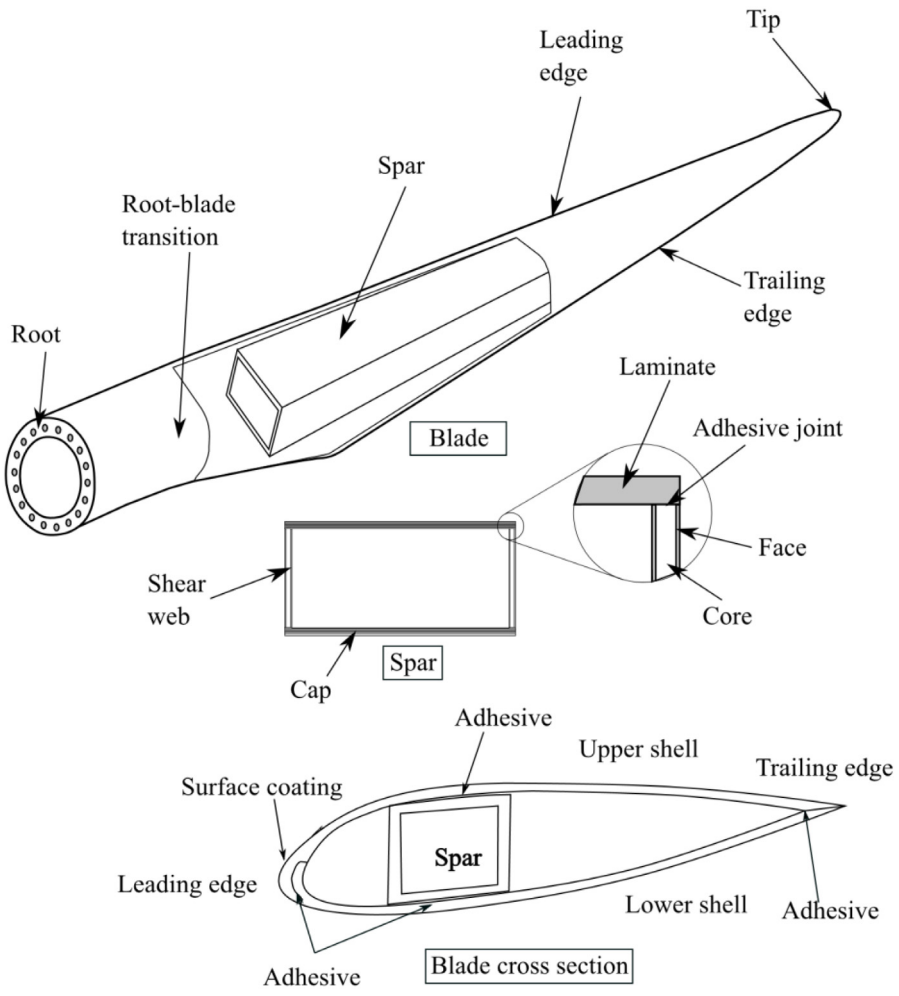

Fig. 2. Wind turbine blade components.

Table 3
Occurrence factor categorization.

Category	Description	Factor
Rare	Remote possibility of failure	1
Unlikely	Relatively few failures	2
Possible	Occasional failures	3
Likely	Repeated failures	4
Almost certain	Almost inevitable failure	5

The proposed maintenance strategies are corrective maintenance, preventive planned maintenance (time-based), preventive condition-based maintenance and predictive condition-based maintenance. The maintenance strategy selection starts with the FMEA of the blade and the determination of the criticality threshold to consider so as to increase the efficiency of the improvements to be implemented. For non-priority failure modes, the corrective maintenance shall be enough since the failure is not so relevant in terms of risk. For those failure modes above the threshold, the feasibility of the monitoring is key to opt for condition-based (either predictive or preventive) or preventive or corrective maintenance. Condition-based maintenance has the advantage of considering the current state of the system. Choosing a predictive maintenance strategy requires the instrumentation of the blade (Martinez-Luengo et al., 2016) and the ability to provide reliable estimations on the future evolution of the failure mode under consideration, which is receiving attention from the research community as shown in Chiachio et al. (2020), while preventive maintenance requires an optimized inspection interval to increase efficiency. For those failure modes that are not able to be monitored, preventive planned maintenance shall be used, when technically and economically feasible, and corrective maintenance otherwise. Finally, if the corrective maintenance is not acceptable due to economic, environmental, safety or other implications, improvements are required to reduce the risk of the failure mode (for example design modifications, improvement of materials or modification of operation).

4. Risk identification and criticality assessment

The identification of risks was performed in consultation with industry experts, of which, its distribution among the different components of the blade is shown in Table 4 and the causes divided in four categories (design, manufacturing, installation and operation) shown in Table 5. A total of 62 failure modes have been identified, being the spar and the upper and lower shells the components with the higher number of failure modes identified, with a total of 20, 11 and 11, respectively.

The spar is the part of the blade having the mission of the structural integrity of the blade and, therefore, its failure modes can evolve until the complete failure of the blade requiring its complete replacement if not maintained in time. The spar is composed of the caps, responsible for the bearing of the flapwise bending loads of the blade, which are the predominant

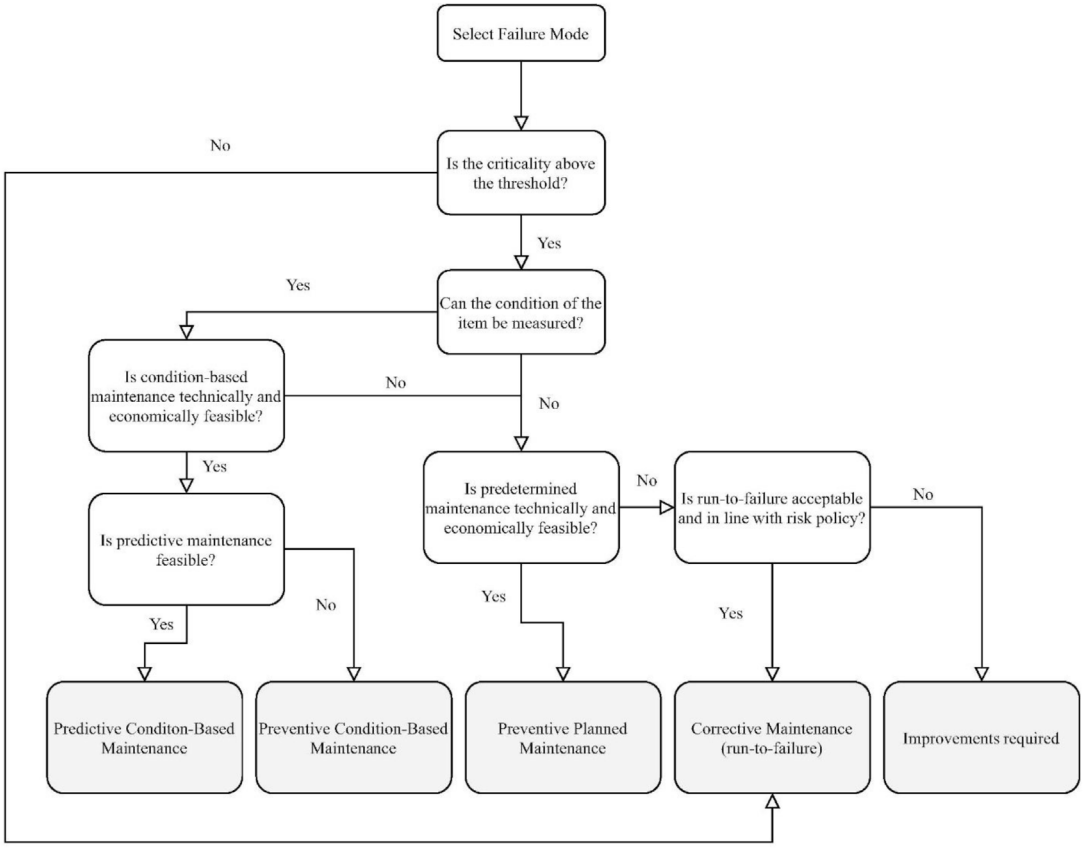

Fig. 3. Maintenance decision tree.
Source: Adapted from Kolios (2020).

Table 4
Identified risks from the FMEA.

Failure mode	LE	LS	R	S	T	TE	US	Grand total
Adhesive joint failure (debonding)	3					3		6
Blade rupturing, blade burnout, wire melting. (Lightning)					1			1
Buckling						1		1
Cracks	1	2		5		1	3	12
Cracks in the gelcoat		1						1
Debonding				2				2
Debonding (laminate to core)		1		1			1	3
Delamination		2		5			2	9
Erosion of leading edge protection (LEP)	3							3
Failure of root-hub connection			3					3
Ice accumulation	1							1
Intralaminar fracture (matrix cracking-microcracks)		3		6			3	12
Receptor vaporization, surface scorching, surface blotching, surface delamination (lightning)					1			1
Skin/adhesive debonding		1					1	2
Surface cracking, surface tearing (lightning)					1			1
Surface stripping, receptor loss (lightning)					1			1
Water ingress		1		1			1	3
Grand total	**8**	**11**	**3**	**20**	**4**	**5**	**11**	**62**

LE: Leading edge LS: Lower shell R: Root S: Spar T: Tip TE: Trailing Edge US: Upper Shell.

loads; and the shear webs, designed to withstand shear loading and edgewise bending. The failure modes present in this part follow the usual damage progression of composite materials (intralaminar cracking–delamination–crack formation), with the severity of each of those failure modes growing with damage growth (Guo et al., 2019). The occurrence of these failure modes provokes effects increasing in severity that include the following: reduction of energy production, increase of dislocations of the blade under operation, rise of stress on the laminates, critical dislocation of the blade (tower hit) and collapse of the blade. The initiation of these failure modes is usually related to defects present in the manufacturing process and fatigue damage accumulated throughout the life of the blade (Alonso-Martinez et al., 2019). Additionally, the disbond of the cap-shear web connection

Table 5
Count of failure modes by cause.

Cause	Count of failure modes
Design	23
Installation	6
Manufacturing	22
Operation	11
Grand total	62

and the water ingress constitute failure modes as well and can contribute to the structural performance degradation of the blade.

The upper and lower shells of the blade provide the aerodynamic design of the blade to maximize lift for energy production and minimize drag. The sandwich panels that conform the shells are coated with a gelcoat providing superior smoothness of the surface and wear protection. The shells are affected by the erosion effects of the rain and the abrasive particles carried in the air. Additional failure modes affecting the shells are related to damage in the sandwich panels forming them (interlaminar cracking, delamination, cracks and debonding between the laminate and the core). The effects of these failure modes are primarily related to a loss of energy production and the modification of the aerodynamic loading that can initiate damage in the spar.

The upper and lower shells are joined together in the leading and trailing edges by means of adhesives. The failure of the adhesive is one of the main failure modes of these parts. The leading edge is more prone to suffer erosion due to the incidence of the flow and is one of the most common failure modes of the blades. The blades located in frost-prone environments are usually equipped with deicing systems to avoid the accumulation of ice on the blade and the failure of these systems increases the mass of the blade and can provoke structural damage and rotor imbalance. Separately, the degradation of the trailing edge can result in the local buckling of the shells.

There are two regions of the blade that are affected by singular failure modes, the root and the tip of the blade. The root of the blade provides the connection of the blade with the hub, and can experience failure modes due to manufacturing defects in the machining of the holes and the assembly of the blade to the hub. The failure modes affecting the root have critical consequences, since the failure of the connection of the blade to the hub can result in the detachment of the blade. Separately, even though the blade has a lightning protection system incorporated, it is sometimes not able to fully protect the blade against lightning strikes and could potentially result in different degrees of damage varying from simple receptor damage that is fixed by a simple replacement to more severe damage modes (surface scorching, surface blotching, delamination, surface cracking, surface tearing and blade rupturing) that could even require the replacement of the whole blade.

In light of the failure modes identified, the recent literature regarding damage detection and monitoring of wind turbine blades has been explored to assess the current feasibility of applying condition-based maintenance strategies, as shown in Table 6. This table summarizes the feature and the monitoring techniques used for the different damage modes covered in this study to shed some light on the potential improvements that could be implemented. In terms of available non-destructive testing or monitoring techniques for the blades, thermography, acoustic emission, ultrasonic guided waves, digital image correlation, optical techniques and vibration analysis are the most used in the literature. The applicability of the different techniques depends on factors such as the accessibility of the damaged component, the detectable size of damage, the type of failure mode and the possibility of embedding or attaching a sensor on the structure or needing to perform the inspection with an external device. The features and monitoring techniques identified are linked with the relevant failure modes as to identify the feasibility of continuous monitoring and propose the most adequate maintenance strategy following the decision chart proposed in Tables 7 to 10.

5. Results & discussion

The results of the FMEA are presented in Tables 7 and 8. Fig. 5 presents a summary of the criticality assessment by blade component based on the FMEA results, so the sum of criticality adds to 1 (or 100%). The results are presented subdividing the total criticality of those failure modes with extreme, high, moderate or low values. No extreme values (CN over 20) have been found in the identified failure modes. This assessment reveals the spar and the leading edge to be the components concentrating the highest criticality (38.2% and 16.9%, respectively) (see Fig. 5). In this sense, leading edge erosion is one of the issues that has captured the attention of the industry due to the loss of production occasioned and the acceleration of degradation of other components of the blade. The structural mission of the spar makes it vital for the performance of the system and is also reflected in the criticality distribution. The blade subcomponent criticality assessment is a relevant result that provides guidance to concentrate design improvement, quality control or maintenance efforts on specific parts of the blade, increasing the efficiency of the actions. In this line, the decision tree presented in Fig. 3 provides a systematic way for selecting the most appropriate maintenance strategy for each failure mode.

The top failure modes of the blade according to this study (refer to Table 11), include the erosion of leading edge protection due to an underestimation in the design stage and the usual operation of the wind turbine, the failure of root-hub connection due to an incorrect pretension applied to the bolts, lightning damage of the blades fostered by an insufficient lightning protection system in the design, the adhesive joint failures of the leading and trailing edges and the crack formation and delamination of the members of the spar.

Leading edge erosion is known to produce annual energy production losses of around 5% after the first few years of operation and has the potential to reach 20%–25% if unmaintained (Sareen et al., 2014). Considering this, the design of durable protective coatings and the identification of the optimum maintenance strategy is of vital importance to reduce operational costs. In this sense, the constant collection and analysis of data can provide good deterioration estimates to find optimum maintenance opportunities. The root-hub connection is also a critical part of the blade since the machining of the holes, the handling and the assembling of the blade are delicate operations and small defects and damage can grow into catastrophic failures since this is the only load path for the blade to transmit loads to the foundations of the turbine. Even though the in-place repair of this connection is usually unfeasible, the early detection of this damage mode can help plan the disassembly and protection of the blade to avoid catastrophic failures. The formation and development of cracks in the spar have the difficulty of progressing unnoticeably for visual inspection techniques under the shells of the blade. Therefore, the advantage of monitoring this part is the reduction of unexpected critical failures of the blade. The debonding of the leading and trailing edges is a failure mode that will reduce the output of energy converted from the wind turbine and potentially produce rotor imbalance and increase the loads onto the blade. Being able to identify the length of the debonding is key to control its growth and plan its maintenance accordingly. Separately, lightning strike impact detection and location can also be helpful in terms of evaluating if inspection or maintenance may be necessary and could avoid the action of unnecessary inspections.

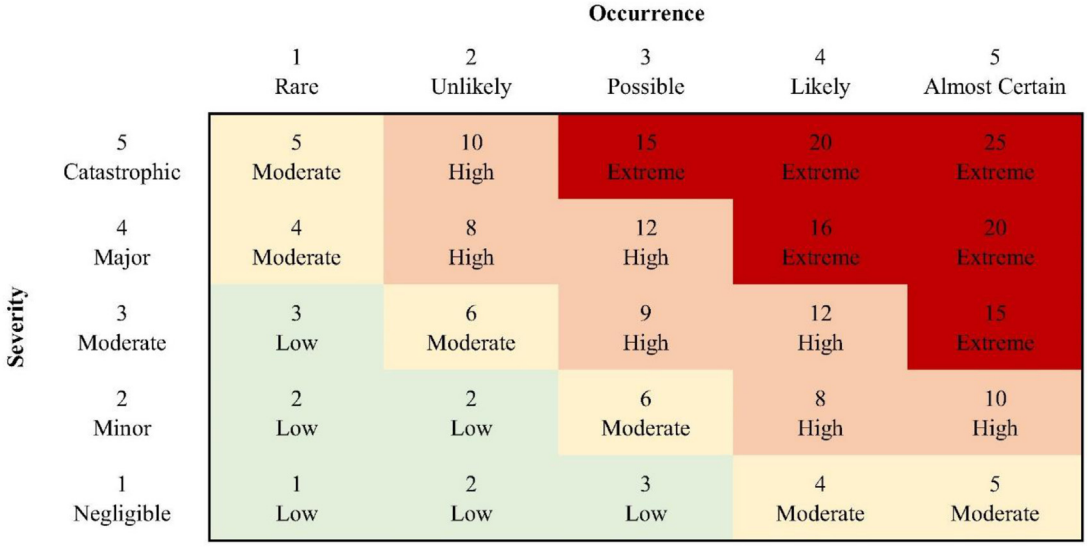

Fig. 4. Criticality matrix.

Table 6
Damage monitoring references in the literature.

Reference	Feature	Monitored damage	Technique
Galleguillos et al. (2015)	Temperature distribution	Delamination, impact, cracks	Thermography
Hwang et al. (2020)	Temperature distribution	Delamination, surface damage	Thermography
Downey et al. (2017)	Strain fields	Cracks	Strain gauges
Gómez Muñoz et al. (2019)	Guided wave amplitude	Delamination in laminates and sandwich parts.	Ultrasonic guided waves.
Solimine et al. (2020)	Signal amplitude	Delamination, cracks	Acoustic emission
Chen et al. (2021)	Temperature distribution, strain fields	Delamination in spar cap, adhesive joint debond, trailing edge buckling.	Thermography, DIC
Park et al. (2014)	Standing wave energy	Trailing edge, leading edge, spar debonding, Delaminations	Ultrasonic guided waves
Skrimpas et al. (2016)	Power curve, tower lateral oscillation acceleration	Ice formation detection	Vibration analysis, power curve analysis
LeBlanc et al. (2013)	Strain and displacement fields	Crack, debonding, delamination	3D DIC
Pereira et al. (2015)	FBG reflectivity-strain	Trailing edge debonding and cracking	Optical (FBG)
Wu et al. (2019)	Strain and displacement fields	Crack, debonding, delamination	3D DIC
Ou et al. (2017)	Natural frequency, damping ratio, mode shapes and curvatures, accelerations	Crack	Vibration analysis
Krause and Ostermann (2020)	AE power and spectral features	Debonding	Acoustic emission
Güemes et al. (2018)	Strain	Debonding and delamination	Optical (FBG)
Haselbach et al. (2016)	Strain and displacement fields	Trailing edge disbond and buckling	Optical (FBG)
Griffith (2015)	Modal shape, frequencies	Trailing edge disbond	Vibration analysis
Zhang et al. (2020)	AE power and amplitude	Cracks	Acoustic emission
Schaal and Mal (2018)	Group wave propagation velocity, energy and amplitude of the wave	Sandwich debonding	Ultrasonic guided waves
Tang et al. (2016)	AE energy, AE amplitude	Matrix cracking, fibre breaking, matrix-fibre debonding	Acoustic emission
Saeedifar et al. (2017)	Time of flight	Delamination	Acoustic emission
Xu et al. (2021)	Amplitude, decay, energy, peak frequency	Matrix cracking, matrix fibre debonding, fibre breakage	Acoustic emission
Matsui et al. (2020)	Wind speed–rotational speed, Wind speed–power	Lightning strike detection	SCADA data analysis
Shihavuddin et al. (2019)	Image analysis aided by deep-learning	Erosion, cracking and lightning	Deep learning
Wang et al. (2019)	Image analysis	Anomaly detection	Deep learning
Kramer et al. (2006)	Current	Lightning impact location	Fibre optic sensor
Tsiapoki et al. (2018)	Natural frequency, damping ratio	Ice formation detection	Vibration analysis
Shoja et al. (2018)	Peak magnitude, group phase velocity	Ice formation detection	Ultrasonic guided waves
Wang et al. (2018)	Amplitude, group phase velocity	Ice formation detection	Ultrasonic guided waves
Sanati et al. (2018)	Temperature distribution	Cracks, delamination, dirt, erosion	Thermography
Ulriksen et al. (2015)	Statistical vibration features	Leading edge and trailing edge cracks	Vibration
Park et al. (2010)	Frequency response functions	Delaminations	Lamb wave propagation
Park et al. (2017)	Time of flight	Delaminations	Ultrasonic guided waves

AE: Acoustic emission DIC: Digital Image Correlation FBG: Fibre Bragg grating SCADA: Supervisory control and data acquisition.

Table 7
FMEA analysis (Failure modes 1 to 31).

ID	Subcomponent level 1	Subcomponent level 2	Subcomponent level 3	Failure mode	Effects	Cause	Cause detail	O	S	CN	Criticality level
LE1	Leading edge	Bondline		Adhesive joint failure (Debonding)	Reduction of aerodynamic efficiency, production losses, separation of the shell, rotor imbalance	Manufacturing	Defective application of adhesive	1	4	4	Moderate
LE2	Leading edge	Bondline		Adhesive joint failure (Debonding)	Reduction of aerodynamic efficiency, production losses, separation of the shell, rotor imbalance	Installation	Damage or overstress of adhesive during handling of the blade	2	4	8	High
LE3	Leading edge	Bondline		Adhesive joint failure (Debonding)	Reduction of aerodynamic efficiency, production losses, separation of the shell	Design	Underestimation of environmental loads and conditions	1	4	4	Moderate
LE4	Leading edge	Skin		Erosion of LEP	Reduction of aerodynamic efficiency, production losses, damage to laminates	Design	Underestimation of wear effects	4	3	12	High
LE5	Leading edge	Skin		Erosion of LEP	Reduction of aerodynamic efficiency, production losses, damage to laminates	Operation	Exposure to UV, rain, insects, salt spray and particle erosion	4	3	12	High
LE6	Leading edge	Skin		Erosion of LEP	Reduction of aerodynamic efficiency, production losses, damage to laminates	Manufacturing	Incorrect curing/application of top coating	3	3	9	High
LE7	Leading edge			Cracks	Exposition of adhesive joint, water ingress	Operation	Excessive loading, fatigue loading	1	3	3	Low
LE8	Leading edge			Ice accumulation	Reduction of aerodynamic efficiency, rotor imbalance, production losses, increase of weight	Operation	Failure of de-icing systems	1	2	2	Low
TE9	Trailing edge	Bondline		Adhesive joint failure (Debonding)	Reduction of aerodynamic efficiency, production losses, separation of the shell	Manufacturing	Defective application of adhesive	1	4	4	Moderate
TE10	Trailing edge	Bondline		Adhesive joint failure (Debonding)	Reduction of aerodynamic efficiency, production losses, separation of the shell, rotor imbalance	Installation	Damage or overstress of adhesive during handling of the blade	2	4	8	High
TE11	Trailing edge	Bondline		Adhesive joint failure (Debonding)	Reduction of aerodynamic efficiency, production losses, separation of the shell	Design	Underestimation of environmental loads and conditions	2	4	8	High
TE12	Trailing edge			Buckling	Collapse of the blade	Design	Underestimation of environmental loads and conditions	1	5	5	Moderate
TE13	Trailing edge			Cracks	Reduction of aerodynamic efficiency, production losses, increase of stress concentration	Design	Underestimation of fatigue loading	2	3	6	Moderate
T14	Tip			Blade rupturing, blade burnout, wire melting (lightning)	Catastrophic damage	Design	Insufficient lightning protection	1	5	5	Moderate
T15	Tip			Surface cracking, Surface tearing (lightning)	Serious damage requiring immediate repair	Design	Insufficient lightning protection	2	4	8	High
T16	Tip			Surface stripping, receptor loss (lightning)	Surface stripping, receptor loss (normal damage)	Design	Insufficient lightning protection	3	3	9	High
T17	Tip			Receptor vaporization, surface scorching, surface blotching surface delamination (Lightning)	Receptor vaporization, surface scorching, surface blotching surface delamination (minor damage)	Design	Insufficient lightning protection	4	2	8	High
R18	Root	Root-hub connection		Failure of root-hub connection	Increase of tension, vibrations of the blade, critical damage of the blade, detachment of blade	Design	Underestimation of environmental/operational loads	1	5	5	Moderate
R19	Root	Root-hub connection		Failure of root-hub connection	Increase of tension, vibrations of the blade, critical damage of the blade, detachment of blade	Manufacturing	Damage to the blade during the machining of the holes	1	5	5	Moderate
R20	Root	Root-hub connection		Failure of root-hub connection	Increase of tension, vibrations of the blade, critical damage of the blade, detachment of blade	Installation	Incorrect pretension applied to the bolts	2	5	10	High
US21	Upper shell	Skin	Gelcoat	Cracks	Increase of water ingress to sandwich and laminates, degradation of properties, loss of stiffness and strength	Design	Insufficient environmental and impact protection	1	1	1	Low
US22	Upper shell	Skin	Skin-laminate interphase	Skin/adhesive debonding	Exposure of laminates to environment, increase of degradation of sandwich composites, reduction of aerodynamic efficiency	Manufacturing	Incorrect application of adhesive	1	2	2	Low
US23	Upper shell	Sandwich	Core	Water ingress	Increase of weight, degradation of stiffness and strength	Design	Degradation of gelcoat exposing laminate and sandwich layers	2	1	2	Low
US24	Upper shell	Sandwich	Laminate-core interphase	Debonding (Laminate to core)	Increase of stress, reduction of stiffness of the sandwich	Manufacturing	Damage during manufacturing, incorrect application of adhesives	2	2	4	Moderate
US25	Upper shell	Sandwich	Laminate	Delamination	Increase of stress concentration, reduction of stiffness, reduction of power	Manufacturing	Voids during manufacturing	2	2	4	Moderate
US26	Upper shell	Sandwich	Laminate	Delamination	Increase of stress concentration, reduction of stiffness, reduction of power	Design	Failure in the design, underestimation of loads	2	2	4	Moderate
US27	Upper shell	Sandwich	Laminate	Intralaminar fracture (matrix cracking-microcracks)	Increase of stress concentration, reduction of stiffness, damage progress to delamination	Manufacturing	Voids in the laminate, fibre misalignment, wrinkles in the fibres	3	1	3	Low
US28	Upper shell	Sandwich	Laminate	Intralaminar fracture (matrix cracking-microcracks)	Increase of stress concentration, reduction of stiffness, damage progress to delamination	Installation	Damage in coating with tools, transportation, and assembly	3	1	3	Low
US29	Upper shell	Sandwich	Laminate	Intralaminar fracture (matrix cracking-microcracks)	Increase of stress concentration, reduction of stiffness, damage progress to delamination	Operation	Incorrect operation resulting in loads not covered by design	3	1	3	Low
US30	Upper shell	Sandwich	Laminate	Cracks	Increase of stress concentration, reduction of stiffness, reduction of power	Design	Underestimation of loads	1	2	2	Low
US31	Upper shell	Sandwich	Laminate	Cracks	Increase of stress concentration, reduction of stiffness, reduction of power	Manufacturing	Voids during manufacturing	1	2	2	Low

O:Occurrence S:Severity CN:Criticality number LEP: Leading edge protection AE: Acoustic emission FBG: Fibre Bragg grating.

Table 8
FMEA analysis (Failure modes 1 to 31).

ID	Subcomponent level 1	Subcomponent level 2	Subcomponent level 3	Failure mode	CN	Criticality level	Failure mechanism	Associated monitoring feature	Associated references	CMS	RMS
LE1	Leading edge	Bondline		Adhesive joint failure (Debonding)	4	Moderate	Overstress of the interphase (peeling stresses), separation of shells	Temperature distribution, strain fields, standing wave energy, FBG reflectivity-strain, AE power and spectral features, strain and displacement fields	Chen et al. (2021), Park et al. (2014), Pereira et al. (2015), Krause and Ostermann (2020), Güemes et al. (2018) and Haselbach et al. (2016)	Regular inspections	Regular inspections
LE2	Leading edge	Bondline		Adhesive joint failure (Debonding)	8	High	Overstress of the interphase (peeling stresses), separation of shells	Temperature distribution, strain fields, standing wave energy, FBG reflectivity-strain, AE power and spectral features, strain and displacement fields	Chen et al. (2021), Park et al. (2014), Pereira et al. (2015), Krause and Ostermann (2020), Güemes et al. (2018) and Haselbach et al. (2016)	Regular inspections	Regular inspections
LE3	Leading edge	Bondline		Adhesive joint failure (Debonding)	4	Moderate	Overstress of the interphase (peeling stresses), separation of shells	Temperature distribution, strain fields, standing wave energy, FBG reflectivity-strain, AE power and spectral features, strain and displacement fields	Chen et al. (2021), Park et al. (2014), Pereira et al. (2015), Krause and Ostermann (2020), Güemes et al. (2018) and Haselbach et al. (2016)	Regular inspections	Regular inspections
LE4	Leading edge	Skin		Erosion of LEP	12	High	Wear of coating, loss of mass of the blade	Temperature distribution, image analysis aided by deep-learning	Hwang et al. (2020), Shihavuddin et al. (2019), Wang et al. (2019) and Sanati et al. (2018)	Regular inspections	Continuous monitoring
LE5	Leading edge	Skin		Erosion of LEP	12	High	Wear of coating, loss of mass of the blade	Temperature distribution, image analysis aided by deep-learning	Hwang et al. (2020), Shihavuddin et al. (2019), Wang et al. (2019) and Sanati et al. (2018)	Regular inspections	Continuous monitoring
LE6	Leading edge	Skin		Erosion of LEP	9	High	Wear of coating, loss of mass of the blade	Temperature distribution, image analysis aided by deep-learning	Hwang et al. (2020), Shihavuddin et al. (2019), Wang et al. (2019) and Sanati et al. (2018)	Regular inspections	Continuous monitoring
LE7	Leading edge			Cracks	3	Low	Degradation and overstress of laminates	Temperature distribution, strain fields, sound signal amplitude, strain and displacement fields, FBG reflectivity-strain, AE power and amplitude, image analysis aided by deep-learning, statistical vibration features	Galleguillos et al. (2015), Solimine et al. (2020), LeBlanc et al. (2013), Pereira et al. (2015), Wu et al. (2019), Zhang et al. (2020), Downey et al. (2017), Hwang et al. (2020), Shihavuddin et al. (2019), Wang et al. (2019), Sanati et al. (2018) and Ulriksen et al. (2015)	Regular inspections	Regular inspections
LE8	Leading edge			Ice accumulation	2	Low	Accumulation of ice	Power curve, tower lateral oscillation acceleration, natural frequency, damping ratio, peak magnitude, group phase velocity, amplitude, group phase velocity	Skrimpas et al. (2016), Tsiapoki et al. (2018), Shoja et al. (2018) and Wang et al. (2018)	Continuous monitoring	Continuous monitoring
TE9	Trailing edge	Bondline		Adhesive joint failure (Debonding)	4	Moderate	Overstress of adhesive	Temperature distribution, standing wave energy, FBG reflectivity-strain, AE power and spectral features, strain and displacement fields, modal shape, frequencies, AE power and amplitude	Chen et al. (2021), Park et al. (2014), Pereira et al. (2015), Krause and Ostermann (2020), Güemes et al. (2018), Haselbach et al. (2016), Griffith (2015) and Zhang et al. (2020)	Regular inspections	Regular inspections
TE10	Trailing edge	Bondline		Adhesive joint failure (Debonding)	8	High	Overstress of the interphase (peeling stresses)	Temperature distribution, strain fields, standing wave energy, FBG reflectivity-strain, AE power and spectral features, strain and displacement fields, modal shape, frequencies	Chen et al. (2021), Park et al. (2014), Pereira et al. (2015), Krause and Ostermann (2020), Güemes et al. (2018), Haselbach et al. (2016) and Griffith (2015)	Regular inspections	Regular inspections
TE11	Trailing edge	Bondline		Adhesive joint failure (Debonding)	8	High	Overstress of adhesive	Temperature distribution, standing wave energy, FBG reflectivity-strain, AE power and spectral features, strain and displacement fields, modal shape, frequencies	Chen et al. (2021), Park et al. (2014), Pereira et al. (2015), Krause and Ostermann (2020), Güemes et al. (2018), Haselbach et al. (2016) and Griffith (2015)	Regular inspections	Regular inspections
TE12	Trailing edge			Buckling	5	Moderate	Overstress of laminate in compression causing buckling instabilities	Temperature distribution, strain and displacement fields	Chen et al. (2021) and Haselbach et al. (2016)	None	None

(*continued on next page*)

Table 8 (*continued*).

ID	Subcomponent level 1	Subcomponent level 2	Subcomponent level 3	Failure mode	CN	Criticality level	Failure mechanism	Associated monitoring feature	Associated references	CMS	RMS
TE13	Trailing edge			Cracks	6	Moderate	Degradation and overstress of laminates	Temperature distribution, sound signal amplitude, strain and displacement fields, FBG reflectivity-strain, AE power and amplitude, image analysis aided by deep-learning, statistical vibration features	Galleguillos et al. (2015), Solimine et al. (2020), LeBlanc et al. (2013), Pereira et al. (2015), Wu et al. (2019), Zhang et al. (2020), Downey et al. (2017), Hwang et al. (2020), Shihavuddin et al. (2019), Wang et al. (2019), Sanati et al. (2018) and Ulriksen et al. (2015)	Regular inspections	Regular inspections
T14	Tip			Blade rupturing, blade burnout, wire melting (lightning)	5	Moderate	Strike of lightning	Wind speed–rotational speed, wind speed–power, image analysis aided by deep-learning, current	Matsui et al. (2020), Shihavuddin et al. (2019), Kramer et al. (2006) and Wang et al. (2019)	Regular inspections	Continuous monitoring
T15	Tip			Surface cracking, Surface tearing (lightning)	8	High	Strike of lightning	Temperature distribution, strain fields, sound signal amplitude, AE power and amplitude, wind speed–rotational speed, wind speed–power, image analysis aided by deep-learning, current	Galleguillos et al. (2015), Hwang et al. (2020), Downey et al. (2017), Solimine et al. (2020), Zhang et al. (2020), Matsui et al. (2020), Shihavuddin et al. (2019), Kramer et al. (2006), Wang et al. (2019) and Sanati et al. (2018)	Regular inspections	Continuous monitoring
T16	Tip			Surface stripping, receptor loss (lightning)	9	High	Strike of lightning	Temperature distribution, wind speed–rotational speed, wind speed–power, image analysis aided by deep-learning, current	Galleguillos et al. (2015), Hwang et al. (2020), Matsui et al. (2020), Shihavuddin et al. (2019), Kramer et al. (2006) and Wang et al. (2019)	Regular inspections	Continuous monitoring
T17	Tip			Receptor vaporization, surface scorching, surface blotching surface delamination (Lightning)	8	High	Strike of lightning	Strain, time of flight, wind speed–rotational speed, wind speed–power, image analysis aided by deep-learning, current, frequency response functions, time of flight	Güemes et al. (2018), Saeedifar et al. (2017), Matsui et al. (2020), Shihavuddin et al. (2019), Kramer et al. (2006), Wang et al. (2019), Park et al. (2010) and Park et al. (2017)	Regular inspections	Continuous monitoring
R18	Root	Root-hub connection		Failure of root-hub connection	5	Moderate	Interlaminar failure, fatigue failure during operation, detachment of the blade	Strain and displacement fields	LeBlanc et al. (2013)	Regular inspections	Regular inspections
R19	Root	Root-hub connection		Failure of root-hub connection	5	Moderate	Interlaminar failure, fatigue failure during operation, detachment of the blade	Strain and displacement fields	LeBlanc et al. (2013)	Regular inspections	Regular inspections
R20	Root	Root-hub connection		Failure of root-hub connection	10	High	Damage progression in the surroundings of the bolts until critical damage of the blade	Strain and displacement fields	LeBlanc et al. (2013)	Regular inspections	Continuous monitoring
US21	Upper shell	Skin	Gelcoat	Cracks	1	Low	Crack initiation due to degradation of properties (UV, impacts), exposing internal layers	Temperature distribution, strain and displacement fields, AE energy, AE amplitude, image analysis aided by deep-learning	Hwang et al. (2020), Downey et al. (2017), LeBlanc et al. (2013), Wu et al. (2019), Tang et al. (2016), Shihavuddin et al. (2019) and Wang et al. (2019)	Regular inspections	Regular inspections
US22	Upper shell	Skin	Skin-laminate interphase	Skin/adhesive debonding	2	Low	Initiation of debonding during operation	Strain and displacement fields, AE power and spectral features	LeBlanc et al. (2013), Wu et al. (2019), Krause and Ostermann (2020) and Güemes et al. (2018)	Corrective maintenance	Corrective maintenance
US23	Upper shell	Sandwich	Core	Water ingress	2	Low	Moisture ingressing slowly and increasing the weight of the blade			Corrective maintenance	Corrective maintenance
US24	Upper shell	Sandwich	Laminate-core interphase	Debonding (Laminate to core)	4	Moderate	Overstress of the interphase (peeling stresses) and fatigue, breathing effects	Temperature distribution, standing wave energy, strain and displacement fields, AE power and spectral features, group wave propagation velocity, energy and amplitude of the wave	Chen et al. (2021), Park et al. (2014), LeBlanc et al. (2013), Wu et al. (2019), Krause and Ostermann (2020), Güemes et al. (2018) and Schaal and Mal (2018)	Corrective maintenance	Corrective maintenance

(*continued on next page*)

Table 8 (*continued*).

ID	Subcomponent level 1	Subcomponent level 2	Subcomponent level 3	Failure mode	CN	Criticality level	Failure mechanism	Associated monitoring feature	Associated references	CMS	RMS
US25	Upper shell	Sandwich	Laminate	Delamination	4	Moderate	Delamination will progress until cracks join and the cross section cannot withstand existing loads	Temperature distribution, guided wave amplitude, sound signal amplitude, standing wave energy, strain and displacement fields, time of flight, frequency response functions	Galleguillos et al. (2015), Hwang et al. (2020), Gómez Muñoz et al. (2019), Solimine et al. (2020), Chen et al. (2021), Park et al. (2014), LeBlanc et al. (2013), Wu et al. (2019), Güemes et al. (2018), Saeedifar et al. (2017), Park et al. (2010) and Park et al. (2017)	Corrective maintenance	Corrective maintenance
US26	Upper shell	Sandwich	Laminate	Delamination	4	Moderate	Intralaminar fractures progressing and evolving into delamination, damage propagation until failure	Temperature distribution, guided wave amplitude, sound signal amplitude, standing wave energy, strain and displacement fields, time of flight, frequency response functions	Galleguillos et al. (2015), Hwang et al. (2020), Gómez Muñoz et al. (2019), Solimine et al. (2020), Chen et al. (2021), Park et al. (2014), LeBlanc et al. (2013), Wu et al. (2019), Güemes et al. (2018), Saeedifar et al. (2017), Park et al. (2010) and Park et al. (2017)	Corrective maintenance	Corrective maintenance
US27	Upper shell	Sandwich	Laminate	Intralaminar fracture (matrix cracking-microcracks)	3	Low	Reduced strength, static or fatigue damage progression	AE energy, AE amplitude, decay, energy, peak frequency	Tang et al. (2016) and Xu et al. (2021)	Corrective maintenance	Corrective maintenance
US28	Upper shell	Sandwich	Laminate	Intralaminar fracture (matrix cracking-microcracks)	3	Low	Reduced strength, static or fatigue damage progression	AE energy, AE amplitude, decay, energy, peak frequency	Tang et al. (2016) and Xu et al. (2021)	Corrective maintenance	Corrective maintenance
US29	Upper shell	Sandwich	Laminate	Intralaminar fracture (matrix cracking-microcracks)	3	Low	Reduced strength, static or fatigue damage progression	AE energy, AE amplitude, decay, energy, peak frequency	Tang et al. (2016) and Xu et al. (2021)	Corrective maintenance	Corrective maintenance
US30	Upper shell	Sandwich	Laminate	Cracks	2	Low	Static and/or fatigue loading	Temperature distribution, sound signal amplitude, strain and displacement fields, FBG reflectivity-strain, AE power and amplitude, image analysis aided by deep-learning	Galleguillos et al. (2015), Hwang et al. (2020), Downey et al. (2017), Solimine et al. (2020), LeBlanc et al. (2013), Pereira et al. (2015), Wu et al. (2019), Zhang et al. (2020), Shihavuddin et al. (2019), Wang et al. (2019) and Sanati et al. (2018)	Corrective maintenance	Corrective maintenance
US31	Upper shell	Sandwich	Laminate	Cracks	2	Low	Static and/or fatigue loading	Temperature distribution, sound signal amplitude, strain and displacement fields, FBG reflectivity-strain, AE power and amplitude, image analysis aided by deep-learning	Galleguillos et al. (2015), Hwang et al. (2020), Downey et al. (2017), Solimine et al. (2020), LeBlanc et al. (2013), Pereira et al. (2015), Wu et al. (2019), Zhang et al. (2020), Shihavuddin et al. (2019), Wang et al. (2019) and Sanati et al. (2018)	Corrective maintenance	Corrective maintenance

CN: Criticality number LEP: Leading edge protection AE: Acoustic emission FBG: Fibre Bragg grating.

Table 9
FMEA analysis (Failure modes 32 to 62).

ID	Subcomponent level 1	Subcomponent level 2	Subcomponent level 3	Failure mode	Effects	Cause	Cause detail	O	S	CN	Criticality level
LS32	Lower shell	Skin	Gelcoat	Cracks in the gelcoat	Increase of water ingress to sandwich and laminates, degradation of properties, loss of stiffness and strength	Design	Insufficient environmental and impact protection	3	1	3	Low
LS33	Lower shell	Skin	Skin-laminate interphase	Skin/adhesive debonding	Exposure of laminates to environment, increase of degradation of sandwich composites, reduction of aerodynamic efficiency	Manufacturing	Incorrect application of adhesive	1	2	2	Low
LS34	Lower shell	Sandwich	Core	Water ingress	Increase of weight, degradation of stiffness and strength	Operation	Degradation of gelcoat, penetration of water	2	1	2	Low
LS35	Lower shell	Sandwich	Laminate-core interphase	Debonding (Laminate to core)	Increase of stress, reduction of stiffness of the sandwich	Manufacturing	Incorrect application of adhesive	2	2	4	Moderate
LS36	Lower shell	Sandwich	Laminate	Delamination	Increase of stress concentration, reduction of stiffness, reduction of power	Manufacturing	Voids during manufacturing	2	2	4	Moderate
LS37	Lower shell	Sandwich	Laminate	Delamination	Increase of stress concentration, reduction of stiffness, reduction of power	Design	Failure in the design, underestimation of loads	2	2	4	Moderate
LS38	Lower shell	Sandwich	Laminate	Intralaminar fracture (matrix cracking-microcracks)	Increase of stress concentration, reduction of stiffness, damage progress to delamination	Manufacturing	Voids in the laminate, fibre misalignment, wrinkles in the fibres	3	1	3	Low
LS39	Lower shell	Sandwich	Laminate	Intralaminar fracture (matrix cracking-microcracks)	Increase of stress concentration, reduction of stiffness, damage progress to delamination	Installation	Damage in coating with tools, transportation, and assembly	3	1	3	Low
LS40	Lower shell	Sandwich	Laminate	Intralaminar fracture (matrix cracking-microcracks)	Increase of stress concentration, reduction of stiffness, damage progress to delamination	Operation	Incorrect operation	3	1	3	Low
LS41	Lower shell	Sandwich	Laminate	Cracks	Increase of stress concentration, reduction of stiffness, reduction of power	Design	Underestimation of loads	1	2	2	Low
LS42	Lower shell	Sandwich	Laminate	Cracks	Increase of stress concentration, reduction of stiffness, reduction of power	Manufacturing	Voids during manufacturing	1	2	2	Low
S43	Spar	Spar-shell connection		Debonding	Increase of blade deformations, increase of stress in shell sandwich members, failure of the blade	Manufacturing	Poor quality or insufficient adhesive bonding between the parts	2	3	6	Moderate
S44	Spar	Spar-shell connection		Debonding	Increase of blade deformations, increase of stress in shell sandwich members, failure of the blade	Operation	Fatigue damage of bonding due to gravitational loads during operation	2	3	6	Moderate
S45	Spar	Caps	Laminate	Delamination	Increase of stress concentration, reduction of stiffness, progress to crack formation	Manufacturing	Voids during manufacturing	2	4	8	High
S46	Spar	Caps	Laminate	Delamination	Increase of stress concentration, reduction of stiffness, progress to crack formation	Design	Failure in the design, underestimation of loads	2	4	8	High
S47	Spar	Caps	Laminate	Delamination	Increase of stress concentration, reduction of stiffness, progress to crack formation	Operation	Incorrect operation, increase of loads	2	4	8	High
S48	Spar	Caps	Laminate	Intralaminar fracture (matrix cracking-microcracks)	Increase of stress concentration, reduction of stiffness, damage progression to delamination	Design	Failure in the design, underestimation of loads	3	2	6	Moderate
S49	Spar	Caps	Laminate	Intralaminar fracture (matrix cracking-microcracks)	Increase of stress concentration, reduction of stiffness, damage progression to delamination	Manufacturing	Voids in the laminate, fibre misalignment, wrinkles in the fibres	3	2	6	Moderate
S50	Spar	Caps	Laminate	Intralaminar fracture (matrix cracking-microcracks)	Increase of stress concentration, reduction of stiffness, damage progression to delamination	Operation	Incorrect operation resulting in loads not covered by design	3	2	6	Moderate
S51	Spar	Caps	Laminate	Cracks	Increase of stress concentration, reduction of stiffness, failure of the blade	Operation	Misoperation, increase of loads	2	5	10	High
S52	Spar	Caps	Laminate	Cracks	Increase of stress concentration, reduction of stiffness, failure of the blade	Design	Underestimation of loads	2	5	10	High

(*continued on next page*)

Table 9 (*continued*).

ID	Subcomponent level 1	Subcomponent level 2	Subcomponent level 3	Failure mode	Effects	Cause	Cause detail	O	S	CN	Criticality level
S53	Spar	Caps	Laminate	Cracks	Increase of stress concentration, reduction of stiffness, failure of the blade	Manufacturing	Voids during manufacturing	2	5	10	High
S54	Spar	Sandwich shear webs	Laminate	Delamination	Increase of stress concentration, reduction of stiffness, progress to crack formation	Manufacturing	Voids during manufacturing	2	4	8	High
S55	Spar	Sandwich shear webs	Laminate	Delamination	Increase of stress concentration, reduction of stiffness, progress to crack formation	Design	Failure in the design, underestimation of loads	2	4	8	High
S56	Spar	Sandwich shear webs	Laminate	Intralaminar fracture (matrix cracking-microcracks)	Increase of stress concentration, reduction of stiffness, damage progress to delamination	Manufacturing	Voids in the laminate, fibre misalignment, wrinkles in the fibres	2	1	2	Low
S57	Spar	Sandwich shear webs	Laminate	Intralaminar fracture (matrix cracking-microcracks)	Increase of stress concentration, reduction of stiffness, damage progress to delamination	Installation	Damage in coating with tools, transportation, and assembly	2	1	2	Low
S58	Spar	Sandwich shear webs	Laminate	Intralaminar fracture (matrix cracking-microcracks)	Increase of stress concentration, reduction of stiffness, damage progress to delamination	Operation	Incorrect operation	2	1	2	Low
S59	Spar	Sandwich shear webs	Laminate	Cracks	Increase of stress concentration, reduction of stiffness, failure of the blade	Design	Underestimation of loads	1	5	5	Moderate
S60	Spar	Sandwich shear webs	Laminate	Cracks	Increase of stress concentration, reduction of stiffness, failure of the blade	Manufacturing	Voids during manufacturing	1	5	5	Moderate
S61	Spar	Sandwich shear webs	Core	Water ingress	Increase of weight, degradation of stiffness and strength	Design	Insufficient environmental and impact protection	1	1	1	Low
S62	Spar	Sandwich shear webs	Laminate-core interphase	Debonding (Laminate to core)	Increase of stress, reduction of stiffness of the sandwich, buckling of the blade	Manufacturing	Incorrect application of adhesive	1	5	5	Moderate

O:Occurrence S:Severity CN:Criticality number LEP: Leading edge protection AE: Acoustic emission FBG: Fibre Bragg grating.

Table 10
FMEA analysis (Failure modes 32 to 62).

ID	Subcomponent level 1	Subcomponent level 2	Subcomponent level 3	Failure mode	CN	Criticality level	Failure mechanism	Associated monitoring feature	Associated references	CMS	RMS
LS32	Lower shell	Skin	Gelcoat	Cracks in the gelcoat	3	Low	Crack initiation due to degradation of properties (UV, impacts), exposing internal layers	Temperature distribution, strain and displacement fields, AE energy, AE amplitude, image analysis aided by deep-learning	Hwang et al. (2020), Downey et al. (2017), LeBlanc et al. (2013), Wu et al. (2019), Tang et al. (2016), Shihavuddin et al. (2019) and Wang et al. (2019)	Corrective maintenance	Corrective maintenance
LS33	Lower shell	Skin	Skin-laminate interphase	Skin/adhesive debonding	2	Low	Initiation of debonding during operation	Strain and displacement fields, AE power and spectral features	LeBlanc et al. (2013), Wu et al. (2019), Krause and Ostermann (2020) and Güemes et al. (2018)	Corrective maintenance	Corrective maintenance
LS34	Lower shell	Sandwich	Core	Water ingress	2	Low	Moisture ingressing slowly and increasing the weight of the blade			Corrective maintenance	Corrective maintenance
LS35	Lower shell	Sandwich	Laminate-core interphase	Debonding (Laminate to core)	4	Moderate	Overstress of the interphase (peeling stresses) and fatigue, breathing effects	Temperature distribution, standing wave energy, strain and displacement fields, AE power and spectral features, group wave propagation velocity, energy and amplitude of the wave	Chen et al. (2021), Park et al. (2014), LeBlanc et al. (2013), Wu et al. (2019), Krause and Ostermann (2020), Güemes et al. (2018) and Schaal and Mal (2018)	Corrective maintenance	Corrective maintenance
LS36	Lower shell	Sandwich	Laminate	Delamination	4	Moderate	Delamination will progress until cracks join and the cross section cannot withstand existing loads	Temperature distribution, guided wave amplitude, sound signal amplitude, standing wave energy, strain and displacement fields, time of flight, frequency response functions	Galleguillos et al. (2015), Hwang et al. (2020), Gómez Muñoz et al. (2019), Solimine et al. (2020), Chen et al. (2021), Park et al. (2014), LeBlanc et al. (2013), Wu et al. (2019), Güemes et al. (2018), Saeedifar et al. (2017), Park et al. (2010) and Park et al. (2017)	Corrective maintenance	Corrective maintenance
LS37	Lower shell	Sandwich	Laminate	Delamination	4	Moderate	Intralaminar fractures progressing and evolving into delamination, damage propagation until failure	Temperature distribution, guided wave amplitude, sound signal amplitude, standing wave energy, strain and displacement fields, time of flight, frequency response functions	Galleguillos et al. (2015), Hwang et al. (2020), Gómez Muñoz et al. (2019), Solimine et al. (2020), Chen et al. (2021), Park et al. (2014), LeBlanc et al. (2013), Wu et al. (2019), Güemes et al. (2018), Saeedifar et al. (2017), Park et al. (2010) and Park et al. (2017)	Corrective maintenance	Corrective maintenance
LS38	Lower shell	Sandwich	Laminate	Intralaminar fracture (matrix cracking-microcracks)	3	Low	Reduced strength, static or fatigue damage progression	AE energy, AE amplitude, decay, energy, peak frequency	Tang et al. (2016) and Xu et al. (2021)	Corrective maintenance	Corrective maintenance
LS39	Lower shell	Sandwich	Laminate	Intralaminar fracture (matrix cracking-microcracks)	3	Low	Reduced strength, static or fatigue damage progression	AE energy, AE amplitude, decay, energy, peak frequency	Tang et al. (2016) and Xu et al. (2021)	Corrective maintenance	Corrective maintenance
LS40	Lower shell	Sandwich	Laminate	Intralaminar fracture (matrix cracking-microcracks)	3	Low	Reduced strength, static or fatigue damage progression	AE energy, AE amplitude, decay, energy, peak frequency	Tang et al. (2016) and Xu et al. (2021)	Corrective maintenance	Corrective maintenance
LS41	Lower shell	Sandwich	Laminate	Cracks	2	Low	Crack formation, failure of the blade	Temperature distribution, sound signal amplitude, strain and displacement fields, FBG reflectivity-strain, strain and displacement fields, AE power and amplitude, image analysis aided by deep-learning	Galleguillos et al. (2015), Hwang et al. (2020), Downey et al. (2017), Solimine et al. (2020), LeBlanc et al. (2013), Pereira et al. (2015), Wu et al. (2019), Zhang et al. (2020), Shihavuddin et al. (2019) and Wang et al. (2019)	Corrective maintenance	Corrective maintenance
LS42	Lower shell	Sandwich	Laminate	Cracks	2	Low	Crack formation, failure of the blade	Temperature distribution, sound signal amplitude, strain and displacement fields, FBG reflectivity-strain, strain and displacement fields, AE power and amplitude, image analysis aided by deep-learning	Galleguillos et al. (2015), Hwang et al. (2020), Downey et al. (2017), Solimine et al. (2020), LeBlanc et al. (2013), Pereira et al. (2015), Wu et al. (2019), Zhang et al. (2020), Shihavuddin et al. (2019) and Wang et al. (2019)	Corrective maintenance	Corrective maintenance

(*continued on next page*)

Table 10 (*continued*).

ID	Subcomponent level 1	Subcomponent level 2	Subcomponent level 3	Failure mode	CN	Criticality level	Failure mechanism	Associated monitoring feature	Associated references	CMS	RMS
S43	Spar	Spar-shell connection		Debonding	6	Moderate	Separation of the spar from the shell, overstress of the interphase (peeling stresses) and fatigue, breathing effects	Temperature distribution, standing wave energy, strain and displacement fields, AE power and spectral features, group wave propagation velocity, energy and amplitude of the wave	Chen et al. (2021), Park et al. (2014), LeBlanc et al. (2013), Wu et al. (2019), Krause and Ostermann (2020), Güemes et al. (2018) and Schaal and Mal (2018)	Corrective maintenance	Continuous monitoring
S44	Spar	Spar-shell connection		Debonding	6	Moderate	Separation of the spar from the shell, overstress of the interphase (peeling stresses) and fatigue, breathing effects	Temperature distribution, standing wave energy, strain and displacement fields, AE power and spectral features, group wave propagation velocity, energy and amplitude of the wave	Chen et al. (2021), Park et al. (2014), LeBlanc et al. (2013), Wu et al. (2019), Krause and Ostermann (2020), Güemes et al. (2018) and Schaal and Mal (2018)	Corrective maintenance	Continuous monitoring
S45	Spar	Caps	Laminate	Delamination	8	High	Delamination will progress until cracks join and the cross section cannot withstand existing loads	Temperature distribution, guided wave amplitude, sound signal amplitude, standing wave energy, strain and displacement fields, time of flight, frequency response functions	Galleguillos et al. (2015), Hwang et al. (2020), Gómez Muñoz et al. (2019), Solimine et al. (2020), Chen et al. (2021), Park et al. (2014), LeBlanc et al. (2013), Wu et al. (2019), Güemes et al. (2018), Saeedifar et al. (2017), Park et al. (2010) and Park et al. (2017)	Corrective maintenance	Corrective maintenance
S46	Spar	Caps	Laminate	Delamination	8	High	Intralaminar fractures progressing and evolving into delamination and damage propagation until failure	Temperature distribution, guided wave amplitude, sound signal amplitude, standing wave energy, strain and displacement fields, time of flight, frequency response functions	Galleguillos et al. (2015), Hwang et al. (2020), Gómez Muñoz et al. (2019), Solimine et al. (2020), Chen et al. (2021), Park et al. (2014), LeBlanc et al. (2013), Wu et al. (2019), Güemes et al. (2018), Saeedifar et al. (2017), Park et al. (2010) and Park et al. (2017)	Corrective maintenance	Corrective maintenance
S47	Spar	Caps	Laminate	Delamination	8	High	Intralaminar fractures progressing and evolving into delamination and damage propagation until failure	Temperature distribution, guided wave amplitude, sound signal amplitude, standing wave energy, strain and displacement fields, time of flight, frequency response functions	Galleguillos et al. (2015), Hwang et al. (2020), Gómez Muñoz et al. (2019), Solimine et al. (2020), Chen et al. (2021), Park et al. (2014), LeBlanc et al. (2013), Wu et al. (2019), Güemes et al. (2018), Saeedifar et al. (2017), Park et al. (2010) and Park et al. (2017)	Corrective maintenance	Corrective maintenance
S48	Spar	Caps	Laminate	Intralaminar fracture (matrix cracking-microcracks)	6	Moderate	Reduced strength and static or fatigue damage progression	AE energy, AE amplitude, decay, energy, peak frequency	Tang et al. (2016) and Xu et al. (2021)	Corrective maintenance	Corrective maintenance
S49	Spar	Caps	Laminate	Intralaminar fracture (matrix cracking-microcracks)	6	Moderate	Reduced strength and static or fatigue damage progression	AE energy, AE amplitude, decay, energy, peak frequency	Tang et al. (2016) and Xu et al. (2021)	Corrective maintenance	Corrective maintenance
S50	Spar	Caps	Laminate	Intralaminar fracture (matrix cracking-microcracks)	6	Moderate	Reduced strength and static or fatigue damage progression	AE energy, AE amplitude, decay, energy, peak frequency	Tang et al. (2016) and Xu et al. (2021)	Corrective maintenance	Corrective maintenance
S51	Spar	Caps	Laminate	Cracks	10	High	Crack formation, failure of the blade	Temperature distribution, Temperature distribution, Strain fields, Sound signal amplitude, Strain and displacement fields, FBG reflectivity-strain, Strain and displacement fields, Natural frequency, damping ratio, mode shapes and curvatures, accelerations, AE power and amplitude	Galleguillos et al. (2015), Hwang et al. (2020), Downey et al. (2017), Solimine et al. (2020), LeBlanc et al. (2013), Pereira et al. (2015), Wu et al. (2019), Ou et al. (2017) and Zhang et al. (2020)	Corrective maintenance	Continuous monitoring

(*continued on next page*)

Table 10 (*continued*).

ID	Subcomponent level 1	Subcomponent level 2	Subcomponent level 3	Failure mode	CN	Criticality level	Failure mechanism	Associated monitoring feature	Associated references	CMS	RMS
S52	Spar	Caps	Laminate	Cracks	10	High	Crack formation, failure of the blade	Temperature distribution, strain fields, sound signal amplitude, strain and displacement fields, FBG reflectivity-strain, natural frequency, damping ratio, mode shape and curvatures, accelerations, AE power and amplitude	Galleguillos et al. (2015), Hwang et al. (2020), Downey et al. (2017), Solimine et al. (2020), LeBlanc et al. (2013), Pereira et al. (2015), Wu et al. (2019), Ou et al. (2017) and Zhang et al. (2020)	Corrective maintenance	Continuous monitoring
S53	Spar	Caps	Laminate	Cracks	10	High	Crack formation, failure of the blade	Temperature distribution, strain fields, sound signal amplitude, strain and displacement fields, FBG reflectivity-strain, natural frequency, damping ratio, mode shape and curvatures, accelerations, AE power and amplitude	Galleguillos et al. (2015), Hwang et al. (2020), Downey et al. (2017), Solimine et al. (2020), LeBlanc et al. (2013), Pereira et al. (2015), Wu et al. (2019), Ou et al. (2017) and Zhang et al. (2020)	Corrective maintenance	Continuous monitoring
S54	Spar	Sandwich shear webs	Laminate	Delamination	8	High	Delamination will progress until cracks join and the cross section cannot withstand existing loads	Guided wave amplitude, sound signal amplitude, temperature distribution, standing wave energy, strain and displacement fields, time of flight, frequency response functions	Gómez Muñoz et al. (2019), Solimine et al. (2020), Chen et al. (2021), Park et al. (2014), LeBlanc et al. (2013), Wu et al. (2019), Güemes et al. (2018), Saeedifar et al. (2017), Park et al. (2010) and Park et al. (2017)	Corrective maintenance	Corrective maintenance
S55	Spar	Sandwich shear webs	Laminate	Delamination	8	High	Intralaminar fractures progressing and evolving into delamination and damage propagation until failure	Guided wave amplitude, sound signal amplitude, temperature distribution, standing wave energy, strain and displacement fields, time of flight, frequency response functions	Gómez Muñoz et al. (2019), Solimine et al. (2020), Chen et al. (2021), Park et al. (2014), LeBlanc et al. (2013), Wu et al. (2019), Güemes et al. (2018), Saeedifar et al. (2017), Park et al. (2010) and Park et al. (2017)	Corrective maintenance	Corrective maintenance
S56	Spar	Sandwich shear webs	Laminate	Intralaminar fracture (matrix cracking-microcracks)	2	Low	Reduced strength and static or fatigue damage progression	AE energy, AE amplitude, decay, energy, peak frequency	Tang et al. (2016) and Xu et al. (2021)	Corrective maintenance	Corrective maintenance
S57	Spar	Sandwich shear webs	Laminate	Intralaminar fracture (matrix cracking-microcracks)	2	Low	Reduced strength and static or fatigue damage progression	AE energy, AE amplitude, decay, energy, peak frequency	Tang et al. (2016) and Xu et al. (2021)	Corrective maintenance	Corrective maintenance
S58	Spar	Sandwich shear webs	Laminate	Intralaminar fracture (matrix cracking-microcracks)	2	Low	Reduced strength and static or fatigue damage progression	AE energy, AE amplitude, decay, energy, peak frequency	Tang et al. (2016) and Xu et al. (2021)	Corrective maintenance	Corrective maintenance
S59	Spar	Sandwich shear webs	Laminate	Cracks	5	Moderate	Crack formation, failure of the blade	Sound signal amplitude, strain and displacement fields, FBG reflectivity-strain, natural frequency, damping ratio, mode shape and curvatures, accelerations, AE power and amplitude	Downey et al. (2017), Solimine et al. (2020), LeBlanc et al. (2013), Pereira et al. (2015), Wu et al. (2019), Ou et al. (2017) and Zhang et al. (2020)	Corrective maintenance	Corrective maintenance
S60	Spar	Sandwich shear webs	Laminate	Cracks	5	Moderate	Crack formation, failure of the blade	Sound signal amplitude, strain and displacement fields, FBG reflectivity-strain, natural frequency, damping ratio, mode shape and curvatures, accelerations, AE power and amplitude	Downey et al. (2017), Solimine et al. (2020), LeBlanc et al. (2013), Pereira et al. (2015), Wu et al. (2019), Ou et al. (2017) and Zhang et al. (2020)	Corrective maintenance	Corrective maintenance
S61	Spar	Sandwich shear webs	Core	Water ingress	1	Low	Moisture ingressing slowly and increasing the weight of the blade			Corrective maintenance	Corrective maintenance
S62	Spar	Sandwich shear webs	Laminate-core interphase	Debonding (Laminate to core)	5	Moderate	Overstress of the interphase (peeling stresses) and fatigue, breathing effects	Group wave propagation velocity, energy and amplitude of the wave	Schaal and Mal (2018)	Corrective maintenance	Corrective maintenance

CN: Criticality number LEP: Leading edge protection AE: Acoustic emission FBG: Fibre Bragg grating.

Table 11
Failure modes with high criticality.

ID	Failure mode	Effects	Cause	Cause detail	Failure mechanism	O	S	CN	Criticality level
LE4	Erosion of LEP	Reduction of aerodynamic efficiency, production losses, damage to laminates	Design	Underestimation of wear effects	Wear of coating, loss of mass of the blade	4	3	12	High
LE5	Erosion of LEP	Reduction of aerodynamic efficiency, production losses, damage to laminates	Operation	Exposure to UV, rain, insects, salt spray and particle erosion	Wear of coating, loss of mass of the blade	4	3	12	High
R20	Failure of root-hub connection	Increase of tension, vibrations of the blade, critical damage of the blade, detachment of blade	Installation	Incorrect pretension applied to the bolts	Damage progression in the surroundings of the bolts until critical damage of the blade	2	5	10	High
S51	Cracks	Increase of stress concentration, reduction of stiffness, failure of the blade	Operation	Misoperation, increase of loads	Crack formation, failure of the blade	2	5	10	High
S52	Cracks	Increase of stress concentration, reduction of stiffness, failure of the blade	Design	Underestimation of loads	Crack formation, failure of the blade	2	5	10	High
S53	Cracks	Increase of stress concentration, reduction of stiffness, failure of the blade	Manufacturing	Voids during manufacturing	Crack formation, failure of the blade	2	5	10	High
LE6	Erosion of LEP	Reduction of aerodynamic efficiency, production losses, damage to laminates	Manufacturing	Incorrect curing/application of top coating	Wear of coating, loss of mass of the blade	3	3	9	High
T16	Surface stripping, receptor loss (lightning)	Surface stripping, receptor loss, normal damage	Design	Insufficient lightning protection	Strike of lightning	3	3	9	High
LE2	Adhesive joint failure (debonding)	Reduction of aerodynamic efficiency, production losses, separation of the shell, rotor imbalance	Installation	Damage or overstress of adhesive during handling of the blade	Overstress of the interphase (peeling stresses), separation of shells	2	4	8	High
TE10	Adhesive joint failure (debonding)	Reduction of aerodynamic efficiency, production losses, separation of the shell, rotor imbalance	Installation	Damage or overstress of adhesive during handling of the blade	Overstress of the interphase (peeling stresses)	2	4	8	High
TE11	Adhesive joint failure (Debonding)	Reduction of aerodynamic efficiency, production losses, separation of the shell	Design	Underestimation of environmental loads and conditions	Overstress of the interphase (peeling stresses)	2	4	8	High
T15	Surface cracking, Surface tearing (lightning)	Serious damage requiring immediate repair	Design	Insufficient lightning protection	Strike of lightning	2	4	8	High
T17	Receptor vaporization, surface scorching, surface blotching and surface delamination (lightning)	Minor damage	Design	Insufficient lightning protection	Strike of lightning	2	4	8	High

(*continued on next page*)

Table 11 (*continued*).

ID	Failure mode	Effects	Cause	Cause detail	Failure mechanism	O	S	CN	Criticality level
S45	Delamination (Caps)	Increase of stress concentration, reduction of stiffness, progress to crack formation	Manufacturing	Voids during manufacturing	Delamination will progress until cracks join and the cross section cannot withstand existing loads	2	4	8	High
S46	Delamination (Caps)	Increase of stress concentration, reduction of stiffness, progress to crack formation	Design	Failure in the design, underestimation of loads	Intralaminar fractures progressing and evolving into delamination, damage propagation until failure	2	4	8	High
S47	Delamination (Caps)	Increase of stress concentration, reduction of stiffness, progress to crack formation	Operation	Incorrect operation, increase of loads	Intralaminar fractures progressing and evolving into delamination, damage propagation until failure	2	4	8	High
S54	Delamination (Shear webs)	Increase of stress concentration, reduction of stiffness, progress to crack formation	Manufacturing	Voids during manufacturing	Delamination will progress until cracks join and the cross section cannot withstand existing loads	2	4	8	High
S55	Delamination (Shear webs)	Increase of stress concentration, reduction of stiffness, progress to crack formation	Design	Failure in the design, underestimation of loads	Intralaminar fractures progressing and evolving into delamination, damage propagation until failure	2	4	8	High

O: Occurrence S: Severity CN: Criticality number LEP: Leading edge protection.

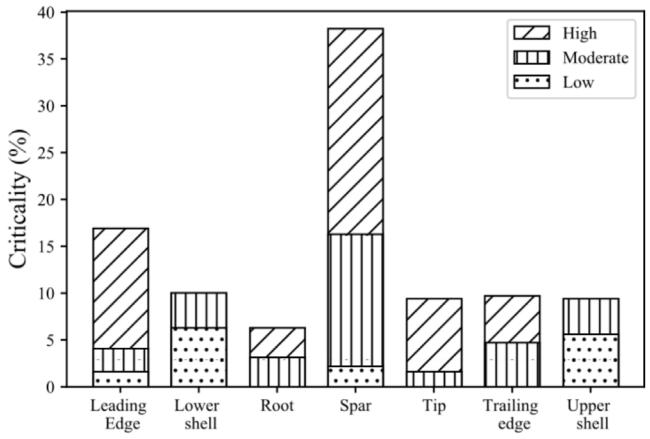

Fig. 5. Criticality by blade component.

The reduction of the Levelized Cost of Energy (LCOE) has been achieved during the last decades, at least partially, with an increase in the size of the turbine and the blades (Mishnaevsky et al., 2017; Sieros et al., 2012). The constant evolution and increase in size of the blades require an understanding of how size and weight increase impact the criticality of the identified failure modes. Overall, the increase in size and the offshore environment to which the turbines are exposed have resulted in a decrease in reliability (Cevasco et al., 2021). In this sense, the levels of stress occasioned by aerodynamic loads can be kept from an excessive growth by increasing the section of the spar, which results in an increase of the mass of the blade, and by the application of both active (primarily based on pitch control) (Griffith et al., 2012; Bossanyi, 2003; Richards et al., 2015; Civelek et al., 2017) and passive (Bortolotti et al., 2019; Chen et al., 2019) load control strategies. Load control strategies may thrive in importance even at the expense of energy production as maintenance costs are higher for offshore wind turbines. The increase of mass of the blade will lead to a rise in the stress, occasioned by the increase in the gravitational and inertial loads. Therefore, the role of both fatigue and extreme damage will grow in importance and those failure modes originated during operation will see their likelihood of occurrence increased and some new failure modes may appear. It is important to note that some fatigue-produced damage is originated from existing manufacturing defects (Marin et al., 2009) and thus, improvement in quality of the manufacturing will also reduce the initiation of these failure modes. Waiting times for weather windows represent a high percentage of these costs, and damage control along with an efficient planning can help to their reduction. Thus, using smart operation control modes can contribute to an overall LCOE reduction if the state of the blade can be known, which grants SHM an additional importance.

6. Conclusion

In this study, a risk-based maintenance strategy selection for wind turbine composite blades was presented. First, the failure modes of the wind turbine blade were identified by means of an FMEA considering their likelihood of occurrence and the severity to determine their criticality. Later, the feasibility of monitoring the identified failure modes was explored in the literature. Finally, a maintenance decision tree was presented and applied to determine the preferred maintenance strategy of the prioritized failure modes providing a systematic way of choosing maintenance strategies for the critical failure modes of the blade.

The FMEA of a wind turbine blade identified the leading edge erosion, root-hub connection damage, spar caps and web damage, lightning strike damage, and the debonding of leading and trailing edges to be the most critical failure modes of the blade. This study has shown that detecting and/or monitoring these failure modes can be feasible as shown by the literature. Notwithstanding, the optimal placement of sensors, the tuning of inspection intervals and dealing with all the information obtained to take operation and maintenance decisions are non-trivial problems to be solved to unleash cost reductions for wind energy production.

CRediT authorship contribution statement

Javier Contreras Lopez: Investigation, Writing – original draft, Writing – review & editing. **Athanasios Kolios:** Conceptualization, Resources, Writing – review & editing, Supervision.

Declaration of competing interest

The authors declare that they have no known competing financial interests or personal relationships that could have appeared to influence the work reported in this paper.

Acknowledgements

This paper is part of the ENHAnCE project that has received funding from the European Union's Horizon 2020 research and innovation programme under the Marie Skłodowska-Curie grant agreement No 859957.

References

Alonso-Martinez, M., Adam, J.M., Alvarez-Rabanal, F.P., del Coz Díaz, J.J., 2019. Wind turbine tower collapse due to flange failure: FEM and DOE analyses. Eng. Fail. Anal. 104, 932–949.

Anthony (Tony) Cox Jr., L., 2008. What's wrong with risk matrices? Risk Anal.: Int. J. 28 (2), 497–512.

Arabian-Hoseynabadi, H., Oraee, H., Tavner, P., 2010. Failure modes and effects analysis (FMEA) for wind turbines. Int. J. Electr. Power Energy Syst. 32 (7), 817–824.

Black, I.M., Richmond, M., Kolios, A., 2021. Condition monitoring systems: a systematic literature review on machine-learning methods improving offshore-wind turbine operational management. Int. J. Sustain. Energy 1–24. http://dx.doi.org/10.1080/14786451.2021.1890736.

Bortolotti, P., Bottasso, C.L., Croce, A., Sartori, L., 2019. Integration of multiple passive load mitigation technologies by automated design optimization—The case study of a medium-size onshore wind turbine. Wind Energy 22 (1), 65–79.

Bossanyi, E.A., 2003. Individual blade pitch control for load reduction. Wind Energy: Int. J. Prog. Appl. Wind Power Convers. Technol. 6 (2), 119–128.

Cevasco, D., Koukoura, S., Kolios, A., 2021. Reliability, availability, maintainability data review for the identification of trends in offshore wind energy applications. Renew. Sustain. Energy Rev. 136, 110414. http://dx.doi.org/10.1016/j.rser.2020.110414.

Chen, X., Semenov, S., McGugan, M., Madsen, S.H., Yeniceli, S.C., Berring, P., Branner, K., 2021. Fatigue testing of a 14.3 m composite blade embedded with artificial defects–damage growth and structural health monitoring. Composites A 140, 106189.

Chen, J., Shen, X., Zhu, X., Du, Z., 2019. Study on composite bend-twist coupled wind turbine blade for passive load mitigation. Compos. Struct. 213, 173–189. http://dx.doi.org/10.1016/j.compstruct.2019.01.086, URL https://www.sciencedirect.com/science/article/pii/S0263822318323754.

Chiachio, J., Jalon, M.L., Chiachio, M., Kolios, A., 2020. A Markov chains prognostics framework for complex degradation processes. Reliab. Eng. Syst. Saf. 195, 106621. http://dx.doi.org/10.1016/j.ress.2019.106621.

Civelek, Z., Lüy, M., Çam, E., Mamur, H., 2017. A new fuzzy logic proportional controller approach applied to individual pitch angle for wind turbine load mitigation. Renew. Energy 111, 708–717. http://dx.doi.org/10.1016/j.renene.2017.04.064, URL https://www.sciencedirect.com/science/article/pii/S0960148117303804.

Corbetta, G., Ho, A., Pineda, I., Ruby, K., Van de Velde, L., Bickley, J., 2015. Wind Energy Scenarios for 2030 Report European Wind Energy Association. Tech. Rep, The European Wind Energy Association, p. 27.

Das, M.K., Panja, S.C., Chowdhury, S., Chowdhury, S.P., Elombo, A.I., 2011. Expert-based FMEA of wind turbine system. In: 2011 IEEE International Conference on Industrial Engineering and Engineering Management. IEEE, pp. 1582–1585.
Dewangan, P., Parey, A., Hammami, A., Chaari, F., Haddar, M., 2020. Damage detection in wind turbine gearbox using modal strain energy. Eng. Fail. Anal. 107, 104228.
Dinmohammadi, F., Shafiee, M., 2013. A fuzzy-FMEA risk assessment approach for offshore wind turbines. Int. J. Progn. Health Manage. 4 (13), 59–68.
Downey, A., Laflamme, S., Ubertini, F., 2017. Experimental wind tunnel study of a smart sensing skin for condition evaluation of a wind turbine blade. Smart Mater. Struct. 26 (12), 125005.
Galleguillos, C., Zorrilla, A., Jimenez, A., Diaz, L., Montiano, A., Barroso, M., Viguria, A., Lasagni, F., 2015. Thermographic non-destructive inspection of wind turbine blades using unmanned aerial systems. Plast. Rubber Compos. 44 (3), 98–103.
2018. Global Wind Report: Annual Market Update 2018. Tech. Rep., URL http://www.gwec.net/wp-content/uploads/2015/03/GWEC_Global_Wind_2014_Report_LR.pdf.
Gómez Muñoz, C.Q., García Márquez, F.P., Hernández Crespo, B., Makaya, K., 2019. Structural health monitoring for delamination detection and location in wind turbine blades employing guided waves. Wind Energy 22 (5), 698–711.
Griffith, D., 2015. Sensing in Renewable Energy Systems: Modal Testing and Structural Health & Prognostics Management. Tech. Rep., Sandia National Lab.(SNL-NM), Albuquerque, NM (United States).
Griffith, D.T., Yoder, N., Resor, B., White, J., Paquette, J., Ogilvie, A., Peters, V., 2012. Prognostic control to enhance offshore wind turbine operations and maintenance strategies. Management 5, 8–10.
Güemes, A., Fernández-López, A., Díaz-Maroto, P.F., Lozano, A., Sierra-Perez, J., 2018. Structural health monitoring in composite structures by fiber-optic sensors. Sensors 18 (4), 1094.
Guo, Y., Yu, L., Wei, X., Liu, W., Huang, X., et al., 2019. Structural collapse characteristics of a 48.8 m wind turbine blade under ultimate bending loading. Eng. Fail. Anal. 106, 104150.
Haselbach, P.U., Eder, M.A., Belloni, F., 2016. A comprehensive investigation of trailing edge damage in a wind turbine rotor blade. Wind Energy 19 (10), 1871–1888.
Hwang, S., An, Y.-K., Yang, J., Sohn, H., 2020. Remote inspection of internal delamination in wind turbine blades using continuous line laser scanning thermography. Int. J. Precis. Eng. Manuf.-Green Technol. 1–14.
IEA, 2020. Projected Costs of Generating Electricity 2020. Tech. Rep., IEA.
International Electrotechnical Commission, et al., 2018. IEC 60812: 2018–Failure Modes and Effects Analysis (FMEA and FMECA), third ed. International Standard. IEC, Geneva, Switzerland.
International Renewable Energy Agency (IRENA), 2021. Renewable Capacity Statistics 2021. Tech. Rep., IRENA, Abu Dhabi.
Kolios, A.J., 2020. Risk-based maintenance strategies for offshore wind energy assets. In: 2020 Annual Reliability and Maintainability Symposium (RAMS). http://dx.doi.org/10.1109/RAMS48030.2020.9153642.
Kolios, A., Martínez-Luengo, M., 2016. The end of the line for today's wind turbines. Renew. Energy Focus 17 (3), 109–111. http://dx.doi.org/10.1016/j.ref.2016.05.003.
Koukoura, S., Scheu, M.N., Kolios, A., 2021. Influence of extended potential-to-functional failure intervals through condition monitoring systems on offshore wind turbine availability. Reliab. Eng. Syst. Saf. 208, 107404. http://dx.doi.org/10.1016/j.ress.2020.107404.
Kramer, S.G., Leon, F.P., Appert, B., 2006. Fiber optic sensor network for lightning impact localization and classification in wind turbines. In: 2006 IEEE International Conference on Multisensor Fusion and Integration for Intelligent Systems. pp. 173–178.
Krause, T., Ostermann, J., 2020. Damage detection for wind turbine rotor blades using airborne sound. Struct. Control Health Monit. 27 (5), e2520.
LeBlanc, B., Niezrecki, C., Avitabile, P., Chen, J., Sherwood, J., 2013. Damage detection and full surface characterization of a wind turbine blade using three-dimensional digital image correlation. Struct. Health Monit. 12 (5–6), 430–439.
Leimeister, M., Kolios, A., 2018. A review of reliability-based methods for risk analysis and their application in the offshore wind industry. Renew. Sustain. Energy Rev. 91, 1065–1076. http://dx.doi.org/10.1016/j.rser.2018.04.004.
Li, H., Teixeira, A.P., Soares, C.G., 2020. A two-stage failure mode and effect analysis of offshore wind turbines. Renew. Energy 162, 1438–1461.
Li, Y., Zhu, C., Song, C., Tan, J., 2018. Research and development of the wind turbine reliability. Int. J. Mech. Eng. Appl. 6 (2), 35–45.
Luengo, M.M., Kolios, A., 2015. Failure mode identification and end of life scenarios of offshore wind turbines: A review. Energies 8 (8), 8339–8354. http://dx.doi.org/10.3390/en8088339.
Magomedov, I.A., Magomadov, V.S., Rahimov, A.A., Alikhadzhiev, S.K., Gudaev, M.A., 2019. FMMA And FMECA for analysis of reliability of a wind turbine. 1399, Institute of Physics Publishing,
Marin, J., Barroso, A., Paris, F., Canas, J., 2009. Study of fatigue damage in wind turbine blades. Eng. Fail. Anal. 16 (2), 656–668.
Martin, R., Lazakis, I., Barbouchi, S., Johanning, L., 2016. Sensitivity analysis of offshore wind farm operation and maintenance cost and availability. Renew. Energy 85, 1226–1236.
Martinez-Luengo, M., Kolios, A., Wang, L., 2016. Structural health monitoring of offshore wind turbines: A review through the statistical pattern recognition paradigm. Renew. Sustain. Energy Rev. 64, 91–105. http://dx.doi.org/10.1016/j.rser.2016.05.085.
Martinez-Luengo, M., Shafiee, M., Kolios, A., 2019. Data management for structural integrity assessment of offshore wind turbine support structures: data cleansing and missing data imputation. Ocean Eng. 173, 867–883. http://dx.doi.org/10.1016/j.oceaneng.2019.01.003.
Matsui, T., Yamamoto, K., Sumi, S., Triruttanapiruk, N., 2020. Detection of lightning damage on wind turbine blades using the SCADA system. IEEE Trans. Power Deliv. 36 (2), 777–784.
Mishnaevsky, L., Branner, K., Petersen, H.N., Beauson, J., McGugan, M., Sørensen, B.F., 2017. Materials for wind turbine blades: An overview. Materials 10 (11), 1–24.
Nejad, A.R., Odgaard, P.F., Gao, Z., Moan, T., 2014. A prognostic method for fault detection in wind turbine drivetrains. Eng. Fail. Anal. 42, 324–336.
Ou, Y., Chatzi, E.N., Dertimanis, V.K., Spiridonakos, M.D., 2017. Vibration-based experimental damage detection of a small-scale wind turbine blade. Struct. Health Monit. 16 (1), 79–96.
Ozturk, S., Fthenakis, V., Faulstich, S., 2018. Failure modes, effects and criticality analysis for wind turbines considering climatic regions and comparing geared and direct drive wind turbines. Energies 11 (9), 2317.
Park, B., An, Y.-K., Sohn, H., 2014. Visualization of hidden delamination and debonding in composites through noncontact laser ultrasonic scanning. Compos. Sci. Technol. 100, 10–18.
Park, B., Sohn, H., Malinowski, P., Ostachowicz, W., 2017. Delamination localization in wind turbine blades based on adaptive time-of-flight analysis of noncontact laser ultrasonic signals. Nondestruct. Test. Eval. 32 (1), 1–20.
Park, G., Taylor, S.G., Farinholt, K.M., Farrar, C.R., 2010. SHM of Wind Turbine Blades Using Piezoelectric Active-Sensors. Tech. Rep., Los Alamos National Lab.(LANL), Los Alamos, NM (United States).
Pereira, G., Mikkelsen, L.P., McGugan, M., 2015. Damage tolerant design and condition monitoring of composite material and bondlines in wind turbine blades: Failure and crack propagation. In: EWEA Offshore 2015 Conference. European Wind Energy Association (EWEA).
Richards, P.W., Griffth, D.T., Hodges, D.H., 2015. Smart loads management for damaged offshore wind turbine blades. Wind Eng. 39 (4), 419–436.
Saeedifar, M., Najafabadi, M.A., Yousefi, J., Mohammadi, R., Toudeshky, H.H., Minak, G., 2017. Delamination analysis in composite laminates by means of acoustic emission and bi-linear/tri-linear cohesive zone modeling. Compos. Struct. 161, 505–512.
Sanati, H., Wood, D., Sun, Q., 2018. Condition monitoring of wind turbine blades using active and passive thermography. Appl. Sci. 8 (10), 2004.
Sareen, A., Sapre, C.A., Selig, M.S., 2014. Effects of leading edge erosion on wind turbine blade performance. Wind Energy 17 (10), 1531–1542.
Schaal, C., Mal, A., 2018. Core-skin disbond detection in a composite sandwich panel using guided ultrasonic waves. J. Nondestruct. Eval. Diagn. Progn. Eng. Syst. 1 (1).
Scheu, M.N., Tremps, L., Smolka, U., Kolios, A., Brennan, F., 2019. A systematic failure mode effects and criticality analysis for offshore wind turbine systems towards integrated condition based maintenance strategies. Ocean Eng. 176, 118–133. http://dx.doi.org/10.1016/j.oceaneng.2019.02.048.
Shafiee, M., Dinmohammadi, F., 2014a. An FMEA-based risk assessment approach for wind turbine systems: a comparative study of onshore and offshore. Energies 7 (2), 619–642.
Shafiee, M., Dinmohammadi, F., 2014b. An FMEA-based risk assessment approach for wind turbine systems: A comparative study of onshore and offshore. Energies 7, 619–642.
Shen, G., Xiang, D., Zhu, K., Jiang, L., Shen, Y., Li, Y., 2018. Fatigue failure mechanism of planetary gear train for wind turbine gearbox. Eng. Fail. Anal. 87, 96–110.
Shihavuddin, A., Chen, X., Fedorov, V., Nymark Christensen, A., Andre Brogaard Riis, N., Branner, K., Bjorholm Dahl, A., Reinhold Paulsen, R., 2019. Wind turbine surface damage detection by deep learning aided drone inspection analysis. Energies 12 (4), 676.
Shoja, S., Berbyuk, V., Boström, A., 2018. Guided wave–based approach for ice detection on wind turbine blades. Wind Eng. 42 (5), 483–495.
Sieros, G., Chaviaropoulos, P., Sørensen, J.D., Bulder, B.H., Jamieson, P., 2012. Upscaling wind turbines: Theoretical and practical aspects and their impact on the cost of energy. Wind Energy 15 (1), 3–17.
Skrimpas, G.A., Kleani, K., Mijatovic, N., Sweeney, C.W., Jensen, B.B., Holboell, J., 2016. Detection of icing on wind turbine blades by means of vibration and power curve analysis. Wind Energy 19 (10), 1819–1832.
Solimine, J., Niezrecki, C., Inalpolat, M., 2020. An experimental investigation into passive acoustic damage detection for structural health monitoring of wind turbine blades. Struct. Health Monit. 19 (6), 1711–1725.
Standard, N., 2001. Criticality analysis for maintenance purposes. Z-008 Rev 2.

Standard, B., Standard, N.Z., 2009a. ISO 31010: RIsk management–Risk assessment techniques. BS ISO 31010.
Standard, B., Standard, N.Z., 2009b. Risk management-principles and guidelines. BS ISO 31000, 2009.
Standard, B., Standard, N.Z., 2015. ISO 2394:2015 GEneral principles on reliability for structures. BS ISO.
Stehly, T.J., Beiter, P.C., 2020. 2018 Cost of Wind Energy Review. Tech. Rep., National Renewable Energy Lab.(NREL), Golden, CO (United States).
Tang, J., Soua, S., Mares, C., Gan, T.-H., 2016. An experimental study of acoustic emission methodology for in service condition monitoring of wind turbine blades. Renew. Energy 99, 170–179.
Tautz-Weinert, J., Watson, S.J., 2016. Using SCADA data for wind turbine condition monitoring–a review. IET Renew. Power Gener. 11 (4), 382–394.
Tsiapoki, S., Häckell, M.W., Grießmann, T., Rolfes, R., 2018. Damage and ice detection on wind turbine rotor blades using a three-tier modular structural health monitoring framework. Struct. Health Monit. 17 (5), 1289–1312.
Ulriksen, M.D., Tcherniak, D., Damkilde, L., 2015. Vibration-based damage identification in wind turbine blades.
Wang, Y., Yoshihashi, R., Kawakami, R., You, S., Harano, T., Ito, M., Komagome, K., Iida, M., Naemura, T., 2019. Unsupervised anomaly detection with compact deep features for wind turbine blade images taken by a drone. IPSJ Trans. Comput. Vis. Appl. 11 (1), 1–7.
Wang, P., Zhou, W., Bao, Y., Li, H., 2018. Ice monitoring of a full-scale wind turbine blade using ultrasonic guided waves under varying temperature conditions. Struct. Control Health Monit. 25 (4), e2138.
Wilburn, D.R., 2011. Wind Energy in the United States and Materials Required for the Land-Based Wind Turbine Industry from 2010 Through 2030. US Department of the Interior, US Geological Survey.
Wu, R., Zhang, D., Yu, Q., Jiang, Y., Arola, D., 2019. Health monitoring of wind turbine blades in operation using three-dimensional digital image correlation. Mech. Syst. Signal Process. 130, 470–483.
Xu, D., Liu, P., Chen, Z., 2021. Damage mode identification and singular signal detection of composite wind turbine blade using acoustic emission. Compos. Struct. 255, 112954.
Zhang, Y., Cui, Y., Xue, Y., Liu, Y., 2020. Modeling and measurement study for wind turbine blade trailing edge cracking acoustical detection. IEEE Access 8, 105094–105103.